

INFORMATION TO USERS

This dissertation was produced from a microfilm copy of the original document. While the most advanced technological means to photograph and reproduce this document have been used, the quality is heavily dependent upon the quality of the original submitted.

The following explanation of techniques is provided to help you understand markings or patterns which may appear on this reproduction.

1. The sign or "target" for pages apparently lacking from the document photographed is "Missing Page(s)". If it was possible to obtain the missing page(s) or section, they are spliced into the film along with adjacent pages. This may have necessitated cutting thru an image and duplicating adjacent pages to insure you complete continuity.
2. When an image on the film is obliterated with a large round black mark, it is an indication that the photographer suspected that the copy may have moved during exposure and thus cause a blurred image. You will find a good image of the page in the adjacent frame.
3. When a map, drawing or chart, etc., was part of the material being photographed the photographer followed a definite method in "sectioning" the material. It is customary to begin photoing at the upper left hand corner of a large sheet and to continue photoing from left to right in equal sections with a small overlap. If necessary, sectioning is continued again — beginning below the first row and continuing on until complete.
4. The majority of users indicate that the textual content is of greatest value, however, a somewhat higher quality reproduction could be made from "photographs" if essential to the understanding of the dissertation. Silver prints of "photographs" may be ordered at additional charge by writing the Order Department, giving the catalog number, title, author and specific pages you wish reproduced.

University Microfilms

300 North Zeeb Road
Ann Arbor, Michigan 48106
A Xerox Education Company

75-4111

GREGORY, Stephen Albert, 1948-
EVOLUTIONARY EFFECTS ON RADIALLY VARYING
PROPERTIES OF COMA CLUSTER GALAXIES.

The University of Arizona, Ph.D., 1974
Astronomy

Xerox University Microfilms, Ann Arbor, Michigan 48106

EVOLUTIONARY EFFECTS ON RADIALLY VARYING PROPERTIES OF
COMA CLUSTER GALAXIES

by

Stephen Albert Gregory

A Dissertation Submitted to the Faculty of the

DEPARTMENT OF ASTRONOMY

In Partial Fulfillment of the Requirements
For the Degree of

DOCTOR OF PHILOSOPHY

In the Graduate College

THE UNIVERSITY OF ARIZONA

1 9 7 4

THE UNIVERSITY OF ARIZONA

GRADUATE COLLEGE

I hereby recommend that this dissertation prepared under my direction by Stephen Albert Gregory entitled Evolutionary Effects on Radially Varying Properties of Coma Cluster Galaxies be accepted as fulfilling the dissertation requirement of the degree of Doctor of Philosophy

William G. Taff
Dissertation Director

6/20/74
Date

After inspection of the final copy of the dissertation, the following members of the Final Examination Committee concur in its approval and recommend its acceptance:*

<u>Gene O'Neil</u>	<u>7/29/74</u>
<u>Ray J. Wayman</u>	<u>6/26/74</u>
<u>William G. Taff</u>	<u>6/20/74</u>
<u>Harold J. Thayer</u>	<u>6/18/74</u>
<u>J. H. S. ...</u>	<u>6/17/74</u>

*This approval and acceptance is contingent on the candidate's adequate performance and defense of this dissertation at the final oral examination. The inclusion of this sheet bound into the library copy of the dissertation is evidence of satisfactory performance at the final examination.

STATEMENT BY AUTHOR

This dissertation has been submitted in partial fulfillment of requirements for an advanced degree at The University of Arizona and is deposited in the University Library to be made available to borrowers under rules of the Library.

Brief quotations from this dissertation are allowable without special permission, provided that accurate acknowledgment of source is made. Requests for permission for extended quotation from or reproduction of this manuscript in whole or in part may be granted by the head of the major department or the Dean of the Graduate College when in his judgment the proposed use of the material is in the interests of scholarship. In all other instances, however, permission must be obtained from the author.

SIGNED:

Stephen A. Gregory

ACKNOWLEDGMENTS

I would like to thank the following members of my family for their support: Terrye Brockman Gregory, my wife, for enabling me to survive graduate school; Floyd E. and Margaret J. Gregory, my parents, and Brent E. Gregory, my brother, for initially stimulating my curiosity.

In addition, I would like to thank the following individuals for helping me professionally: Dr. William G. Tifft for a vast amount of advice and encouragement; Leo P. Connolly and Keith H. Johnson for many discussions and many nights of companionship while observing; Laird A. Thompson for much discussion and for suggesting the numerical morphological classification system that I use; Dr. J. P. Ostriker for an extremely informative afternoon talk; Dr. Ray J. Weymann for advice and generous provision of telescope time.

TABLE OF CONTENTS

	Page
LIST OF TABLES	vi
LIST OF ILLUSTRATIONS	vii
ABSTRACT	viii
 CHAPTER	
1. INTRODUCTION	1
Objectives	3
2. NEW OBSERVATIONS	5
Cluster Membership	15
Radial Dependence of Redshifts	17
Velocity Dispersion	18
Rotation	21
Morphology of Cluster Galaxies	24
Galaxy Colors	25
3. THEORY	28
Observable Effects of Age Differences	38
The Radial Coordinate	38
Effects of a Less Dense Background	39
Gott's Models	40
Radial Mixing	42
4. DISCUSSION	44
The Importance of Faint Members and Nonmembers	44
The Kinetic Energy of Rotation	46
The Dependence of Galaxy Morphology on Cluster Position	48
The Possible Change in Color with Distance	50
Conclusion	54
Suggestions for Further Observations	54

TABLE OF CONTENTS--Continued

	Page
APPENDIX A: NEW REDSHIFT DETERMINATIONS	57
APPENDIX B: MORPHOLOGY AND COLORS	63
REFERENCES	69

LIST OF TABLES

Table	Page
1. Main Table of Observations	7
2. σ_v vs. R	19
3. Morphology vs. R	26
4. Color vs. R	27
5. Summary of Redshift Results	46
6. Rest Wavelengths	58
7. Internal Comparison of Redshifts	61
8. Comparison of Redshifts with Other Observatories	61
9. Calibration of Colors	68

LIST OF ILLUSTRATIONS

Figure		Page
1.	Redshift vs. Apparent Radial Distance	16
2.	Velocity Dispersion vs. Radius	20
3.	Redshift vs. Projected Distance	22
4.	Perturbation Density vs. Radius	32
5.	Average Density Within r	34
6.	Time of Collapse vs. Radius	35

ABSTRACT

A sample of galaxies brighter than $m_p = 15.7$ out to a radial distance of 2.79^0 from the Coma cluster center is essentially completed by new observations of redshifts, morphology, and color. The redshift results show that the velocity dispersion first decreases and then increases again with distance from the center. The mean velocity dispersion is found to be 712 Km sec^{-1} in the line of sight. A marginally positive test for solid body rotation of $86 \pm 66 \text{ Km sec}^{-1} \text{ degree}^{-1}$ is also found. The morphology and color data show two interesting features. First, the relative number of spiral and irregular galaxies is shown to increase with radial distance. Secondly, E and SO galaxies located far from the cluster center appear to be bluer than those near the center.

These observations are discussed in terms of two theories of cluster formation and are shown to be consistent with numerical models of the collapse of axisymmetric rotating systems in which star formation had already occurred at the time of maximum cluster radius. The results are also consistent with the existence of an intracluster medium which forms SO's out of spiral galaxies and reddens the central galaxies by a few hundredths of a magnitude in B-V.

CHAPTER 1

INTRODUCTION

Coma, centered at $12^{\text{h}} 57.4^{\text{m}}, + 28^{\circ} 14.5'$ (1950), is the best studied large cluster of galaxies. It is number 1656 in Abell's (1958) catalogue and is given distance class 1, richness class 2, and magnitude 13.5 (photored magnitude of the tenth brightest member). The mean cluster redshift is about 6900 km sec^{-1} giving a distance modulus of $m-M = 34.8$ magnitudes and a distance of 92 Mpc if Hubble's parameter, H , is $75 \text{ Km sec}^{-1} \text{ Mpc}^{-1}$. At this distance one degree of arc corresponds to about 1.6 Mpc. The large velocity dispersion of the member galaxies indicates a Virial mass discrepancy of almost an order of magnitude. Bautz and Morgan (1970) classify the cluster as Type II--intermediate between those clusters dominated by a cD galaxy and those with no dominant galaxies. Rood and Sastry (1971) classify it as B referring to the fact that the two brightest galaxies near the center, NGC 4889 and NGC 4874, seem to form a binary system. The North Galactic Pole is located within the boundaries of the cluster, and there is negligible galactic absorption.

Determinations of the cluster radius are conflicting. This is especially true of studies based on number count data because of the difficulty in determination of the background level. Zwicky (1957) finds a radius of six degrees. Abell (1962) gives 2.5 degrees, and Omer, Page

and Wilson (1965) find a radius of 1.7 degrees. Studies that involve redshift data give less conflicting radii. Rood et al. (1972, hereafter referred to as RPKK) and Tifft and Gregory (1972) have shown that a large number of galaxies out to a distance of six degrees show redshifts consistent with those of the central regions. Although the central regions are roughly spherical, the outer parts are definitely elongated east-west. This is also the direction of separation of NGC 4889 and NGC 4874. Rood and Sastry (1971) also point out that the direction of elongation points towards the nearby rich cluster A1367 and suggest that the two clusters form a supercluster.

Extensive data has been given for some galaxy properties. Rood and Baum (1967, 1968) derived total Visual magnitudes for about 300 galaxies near the center of the cluster. A more detailed study of the same material including a correction at low light levels is being prepared by Tifft et al. (1974). Philip and Sanduleak (1969) derived a semi-quantitative color parameter for the nuclear regions of many Coma galaxies by inspection of objective prism plates. They covered most galaxies brighter than magnitude 15.5 out to a radius of about two degrees. A large number of redshifts are now also known. In addition to the sources upon which the RPKK study was based and Tifft and Gregory's data, a large sample of redshifts in the central regions is given in a series of papers by Tifft (1972a, 1972b, 1973a). In these and related papers, Tifft finds a relation between luminosity and redshift and suggests that an expanding universe model might be fundamentally incorrect since the entire Doppler redshift concept is questioned.

In the 5C4 radio survey, Willson (1970) finds 189 sources at 408 Mhz within about two degrees of the Coma center but suggests that most of these are field objects. Only 14 are identified with cluster members brighter than $m_p = 17$. He also believes that the extended source associated with NGC 4869 is caused by interactions between the galaxy and relativistic particles ejected by NGC 4874. Welch and Sastry (1971) have given independent support for this hypothesis by finding diffuse luminous material enveloping NGC 4889 and NGC 4874 and extending southwest towards NGC 4869 for 16 minutes of arc. Additional evidence of intense activity is the discovery of a diffuse x-ray source centered near the adopted cluster center. Gursky's (1973) review gives a thermal model with the gas being heated by relativistic electrons from active galaxies the most weight. This source extends over about 1 Mpc and has a luminosity of 4.5×10^{44} ergs sec⁻¹.

Objectives

Although the center of Coma has been studied in considerable detail, much less is known about the surroundings. Some studies mentioned above did cover a wide area of the cluster, but it was not until 1972 in the RPKK paper that a thorough effort was made to integrate data throughout the cluster and account for the dynamics of the cluster as a whole. Such an effort was possible at that time because of the increased availability of fast low dispersion spectrographs with image intensifying devices.

The purpose of this dissertation is to further examine the important properties redshift, morphological type, color, and luminosity

for galaxies in the outer parts of the Coma cluster. Consideration of these observations along with studies already in the literature will help us better understand both the present condition of the cluster and the gross features of its formation.

CHAPTER 2

NEW OBSERVATIONS

Several important prerequisites had to be fulfilled by the sample of galaxies that were to be observed. First, the galaxies had to be chosen without any selection effects caused by position in the cluster. Secondly, the number of galaxies must be large enough that the data would not be unduly influenced by chance statistical fluctuations. Finally, the galaxies had to be bright enough that a large number could be observed.

These criteria were very well met by the galaxies listed individually in the Catalogue of Galaxies and Clusters of Galaxies (hereafter referred to as CGCG, Zwicky and Herzog 1963). Over two hundred galaxies brighter than $m_p = 15.7$ are given in the Coma region out to a radius of three degrees. In an area this small, the faint limit is probably independent of position. However, the quoted magnitude refers to light emitted from all parts of the galaxy and does not necessarily guarantee that the nuclear regions are bright enough for spectroscopic observations.

Besides fitting the criteria very well, an additional attractive feature of this sample is that more than one hundred of the galaxies already have redshift determinations. Most of these are summarized in RPKK. The rest are given by Tifft and Gregory (1972) or in the series

of papers by Tifft that were mentioned in the first chapter (although Tifft went to a much fainter limit in the center of the cluster, and his papers therefore include many galaxies beyond the scope of the present investigation).

A clear goal of the new observations was to complete the redshift determinations to as large a radius as possible. As a result, the sample is now essentially complete to a radius of 2.79 degrees. Five galaxies were either not observed or had spectra too faint to measure, and several companions in multiple systems were too faint. Although several galaxies lying beyond 2.79 degrees have previously been observed, for the sake of internal completeness these are generally not included in the present study.

Table 1 lists the relevant data for all galaxies in this sample. Column 1 gives the identification number. The first 54 galaxies have two-digit numbers preceded by the letter C; these are located in the densely populated central region of the cluster and are listed separately in CGCG. The remaining objects have six-digit numbers with the first three digits giving the field number used in CGCG and the last three digits running sequentially; gaps in the numbers are a result of the fact that CGCG lists galaxies in order of increasing R.A.--some lie beyond the 2.79 degree limit used here. The second column gives alternate identifications (N = NGC, I = IC, RB = Rood and Baum, CT galaxies are from Tifft and Gregory, and A galaxies are from Mayall's (1960) sample). Columns 3, 4, and 5 give the right ascension, declination (both 1950.0) and m_p respectively as listed in CGCG. Column 6 is the

Table 1. Main Table of Observations.

ID	I(alt.)	R.A. (1950)	Dec. (1950)	m_p	R	M	Color	V_o	Source
C 1	I 3946	12 ^h 56 ^m .4	28 ^o 05'	15.3	0.28	1	B	6009	C
C 2	I 3947	56.4	28 04	15.6	0.28	1	B	5700	C
C 3	I 3949	56.5	28 06	14.9	0.25	2	B	7419	C
C 4	N 4858	56.6	28 23	15.5	0.24	2	VB	9398	A
C 5		56.6	28 30	15.3	0.31	2	R		
C 6	N 4860	56.7	28 24	14.7	0.25	2	R	7858	A
C 7	I 3955	56.7	28 16	15.6	0.17	1 _p	N	7687	C
C 8	I 3957	56.7	28 02	15.6	0.27	1	N	6317	C
C 9	I 3959	56.7	28 03	15.2	0.25	1	N	7006	C
C 10	I 3960	56.7	28 08	15.5	0.20	2	N	6679	C
C 11	I 3963	56.8	28 03	15.7	0.24	2	N	6645	C
C 12	N 4864	56.8	28 15	14.8	0.14	1 _p	R	6769	C
C 13	N 4867	56.8	28 14	15.5	0.15	1	N	4827	A
C 14	RB 268	56.8	28 21	15.6	0.18	2	B	7808	C
C 15	N 4865	56.9	28 21	14.6	0.16	2	N	4655	A
C 16	N 4869	56.9	28 11	14.9	0.12	2	B	6801	C
C 17	I 3976	57.0	28 07	15.5	0.15	2	N	6777	C
C 18	N 4871	57.1	28 14	15.1	0.08	2	R	6757	C
C 19	I 3973	57.1	28 09	15.2	0.12	2	N	4732	K
C 20	N 4873	57.1	28 15	15.4	0.08	1	R	5649	K
C 21	N 4872	57.1	28 13	15.3	0.06	2	N	7258	C
C 22	N 4874	57.2	28 14	13.7	0.06	1	VR	7181	C
C 23	N 4875	57.2	28 11	15.6	0.08	1	N	7866	C
C 24	RB 43	57.3	28 12	15.7	0.05	1	N	6809	C
C 25	N 4876	57.3	28 11	15.1	0.07	1	N	6739	C
C 26	RB 49	57.4	28 08	15.6	0.11	4	B	8037	C
C 27	I 3998	57.4	28 15	15.6	0.01	2	R	9358	K
C 28	N 4883	57.5	28 18	15.2	0.06	1	R	8052	C
C 29	N 4881	57.6	28 31	14.7	0.28	2	N	6725	C
C 30	N 4886	57.7	28 15	15.1	0.06	2	N	6227	A
C 31		57.7	28 05	15.7	0.17	2	R		
C 32	N 4889	57.7	28 15	13.0	0.06	2	VR	6521	C
C 33	I 4011	57.7	28 16	15.6	0.06	1	B	7112	C
C 34A	RB 82	57.7	28 08		0.12	1	B	5121	C
C 34B	RB 83					2	B	9875	C

Table 1, Continued. Main Table of Observations.

ID	I(alt.)	R.A. (1950)	Dec. (1950)	m_p	R	M	Color	V_o	Source
C 35	I 4012	12 ^h 57 ^m .7	28 ^o 21'	15.7	0.12	1	N	7248	C
C 36	RB 167	57.8	28 26	15.6	0.20	2	R	6771	A
C 37	I 4021	57.8	28 18	15.6	0.11	1	R	5802	A
C 38	N 4894	57.9	28 14	15.7	0.10	4	B	4557	C
C 39E	N 4898E	57.9	28 14		0.10	1	R	6509	C
C 39W	N 4898W					1	R	6812	C
C 40	N 4895	57.9	28 28	14.3	0.25	4	N	8420	A
C 41	I 4026	58.0	28 19	15.5	0.14	2	N	8198	C
C 42		58.2	28 25	15.7	0.18	4	N		
C 43	I 4040	58.2	28 20	15.1	0.18	2	VB	7644E	A,CR
C 44	N 4906	58.2	28 12	15.2	0.20	2	N	7510	C
C 45	I 4041	58.3	28 16	15.7	0.19	2	R	7087	C
C 46	I 4042	58.3	28 14	15.5	0.19	3	R	6243	K
C 47	I 4045	58.4	28 21	15.1	0.24	2	N	6865	C
C 48	N 4907	58.4	28 26	14.6	0.28	5	VB	5868	A
C 49	N 4908	58.4	28 19	14.9	0.22	2	R	8851	A
C 50	I 4051	58.5	28 16	14.8	0.23	2	N	4945	A
C 51	N 4911	58.5	28 04	13.7	0.31	6	B	8006	A
C 52	RB 124	58.6	28 10	15.6	0.26	4	R	6917	C
130004		13 ^h 01 ^m .3	26 21	15.7	2.08	5		11206E	G
130006		13 ^h 02 ^m .8	26 13	15.0	2.35	5		6542	K
159078	N 4692	12 ^h 45 ^m .4	27 30	14.0	2.76	1		7912	A [1]
079	A 3	45.9	27 08	15.2	2.79	4		6917	A
083	A 4	47.2	27 10	14.9	2.51	3		7430	A
085	N 4715	47.4	28 05	15.4	2.22	3		6902	K
086	N 4721	47.8	27 36	15.2	2.23	4		7858	G
087	N 4728	48.0	27 43	15.6	2.15	2		6526	A
089	A 5	48.3	28 06	14.8	2.02	2		7572	CR,CT
090		48.5	27 39	15.5	2.06	5		8355E	G
091	N 4735	48.6	29 12	15.1	2.16	6		6650E	G,CR
092	N 4738	48.7	29 04	14.9	2.09	5		4801	G
093		48.8	27 23	15.3	2.10	6		5445	CR
094	N 4745	48.9	27 42	15.4	1.96	1		7597	G
097		49.6	27 18	15.4	1.98	1		6546	G
098		49.6	27 51	15.5	1.78	1		8188	G

Table 1, Continued. Main Table of Observations.

ID	I(alt.)	R.A. (1950)	Dec. (1950)	m_p	R	M	Color	V_o	Source
099		12^h 50 ^m .1	27° 01'	15.7	2.04	4		7981	G
100	I 831	50.2	26 45	15.5	2.19	1		6364	G
101		50.3	27 40	15.3	1.68	1		7855E	CR
102		50.4	28 39	14.5	1.60	4		7112	K
104	A 8	50.7	27 21	15.0	1.74	3		6154	CR
105	I 832	51.4	26 43	15.0	2.03	2		7003	CR
106		51.4	29 15	15.6	1.67	4		7890	G
107		51.4	29 51	15.3	2.08	5		13861	G
109		51.6	27 25	14.9	1.53	7			
110		51.6	29 52	14.8	2.07	4		6529	G
111	N 4787	51.7	27 20	15.5	1.56	4		7636	G
112	N 4788	51.8	27 35	15.4	1.41	2		6462	G
113	N 4789	51.9	27 20	13.3	1.53	2		8377	A
114		52.1	28 39	15.5	1.24	5		7132	G
115		52.2	27 12	15.6	1.56	4		6203	G
116	N 4793	52.2	29 12	12.3	1.50	3		2544	A
118	N 4798	52.5	27 41	14.3	1.23	1		7680	A
119		52.5	28 41	15.7	1.17	1		7503	G
160015		53.0	26 05	15.5	0.99	2		7443	G
016		53.0	28 44	15.7	1.09	1		7185	G
160017	N 4807	53.1	27 47	14.4	1.06	1		6853	K [2]
018		53.1	27 56	15.3	1.01	2		7092	G
019	I 3900	53.3	27 31	14.8	1.17	1		7178	A
020		53.7	27 57	15.5	0.88	1		(7424)	G
021	N 4816	53.8	28 01	14.8	0.84	3	R	6862	K
022	CT 29	54.0	26 38	15.2	1.78	1	N	6292	CT
023		54.0	28 01	15.5	0.79	1	N	7100	G
024	N 4821	54.1	27 13	15.0	1.26	1	N	6980	A
025	N 4819	54.1	27 15	14.0	1.24	4	VB	6702	A
026	I 3913	54.1	27 33	15.5	1.01	6	VB		
027		54.1	28 06	15.6	0.75	1	N	6671	G
028	I 4827	54.3	27 26	14.1	1.07	1	N	7657	RC
029	I 4828	54.3	28 17	15.4	0.69	2	R	6141	G
031		54.4	27 22	15.7	1.10	1	N	6852	G
032	I 835	54.5	26 45	14.9	1.63	2	VB	7747	CT

Table 1, Continued. Main Table of Observations.

ID	I(alt.)	R.A. (1950)	Dec. (1950)	m_p	R	M	Color	V_o	Source
160033		12 ^h 54 ^m .5	27 ^o 10'	15.1	1.26	1	B	6282E	CR
034		54.5	29 12	15.2	1.16	4	B	8030	G
035		54.6	29 19	15.4	1.24	2	N	7528	G
037		54.8	27 44	15.0	0.78	1	N	7341	G
038	A 11	54.8	29 18	14.8	1.21	4	N	7472	K
039	N 4839	55.0	27 46	13.6	0.72	1	N	7455	A
040		55.0	27 49	15.3	0.69	1	N	5523	G
041	I 837	55.1	26 46	15.4	1.56	2	B	7041	G
042	N 4840	55.1	27 53	14.8	0.63	1	N	5792E	CR
043		55.1	28 28		0.56	2	N	7078	G
044A	N 4841A	55.1	28 45		0.72	1	N	6708	K
044B	N 4841B					1	R		
045		55.2	27 07	15.5	1.23	2	N	6514	G
046A	N 4842A	55.2	27 45		0.70	1	N	7521	A
046B	N 4842B					1	N		
047		55.3	28 06	15.7	0.49	4	N	6163	G
048A		55.3	28 09		0.48	1	B	6044	G
048B						1	N	6948	G
049		55.4	28 27	15.5	0.50	1	N	(7393)	G
050		55.4	29 55	15.2	1.73	5	VB	(5319)	G
051		55.6	27 08	15.2	1.18	3	N	7371	G
052		55.6	27 11	15.5	1.13	1	B	7979	G
053		55.6	28 05	15.7	0.44	1	B	7205	G
055	N 4848	55.7	28 31	14.2	0.47	5	VB	7221	A
056	N 4949	55.8	26 40	14.5	1.62	1	N	5928	A,CT [3]
057		55.8	28 24	15.5	0.40	2	R	7414	G
058		55.8	28 59	15.5	0.83	7	VB	(7692)	G
059		55.8	29 13	15.2	1.04	2	N	7572	G
061A	N 4851	55.9	28 25		0.38	1	B	7794	G
061B	I 839					1	B	6682	G
062A		55.9	29 24		1.21	2	VB	7850	G
062B						4	VB		
063	N 4850	56.0	28 14	15.3	0.32	3	B	5995	A
064		56.1	27 31	15.4	0.78	7	VB	7425E	CR
065	RB 241	56.1	28 17	15.0	0.30	3	B	7185	C

Table 1, Continued. Main Table of Observations.

ID	I(alt.)	R.A. (1950)	Dec. (1950)	m_p	R	M	Color	V_o	Source
160066		12 ^h 56 ^m .2	27 ^o 22 [']	15.3	0.92	1	N	(7872)	G
067	A 12		56.2 27 26	15.4	0.85	7	VB	7712E	CR
068	N 4853		56.2 27 51	14.2	0.48	1	B	7560	A
069	I 3943		56.2 28 23	15.6	0.31	2	R	6827	G
070	N 4854		56.4 27 57	15.2	0.37	3	R	8240	C
071	N 4859		56.6 27 05	14.8	1.17	1	N	7037	K
073	A 11		56.7 27 55	15.1	0.36	3	VB	5366E	K
074			56.8 27 40	15.4	0.59	3	B	5633	G
076			57.2 28 54	15.6	0.66	5	VB	5342E	CR
077	I 3990		57.2 29 10	15.0	0.93	2	B	6208	K
078	I 3991		57.2 29 12	15.5	0.96	3	N	5914	G
079			57.3 27 58	15.1	0.28	2	B	8219	K
081	N 4892		57.6 27 10	14.7	1.08	2	B	5881	K
082			57.8 27 39	15.6	0.60	7	VB	10871E	G
083			57.8 29 06	15.4	0.86	1	B	7399	G
084			58.0 26 56	15.2	1.31	4	B	7212	G
085	I 4032		58.0 29 08	15.4	0.90	1	RCBH	6787	G
086			58.1 27 55	15.4	0.36	7	VB	7508E	CR
087	N 4896		58.1 28 37	15.1	0.40	1	R	5834	A
088	I 842		58.2 29 17	14.6	1.05	5	VB	7193	G
089			58.3 28 36	15.6	0.40	1	B	8008	G2
090			58.4 27 40	15.5	0.61	4	B	6932	G
091	A 14		58.5 28 38	14.9	0.45	1	N	7695	K
092			58.7 28 05	15.7	0.32	1	B	5986	G
093			58.8 28 04	15.7	0.35	1	N	6522	G
094	N 4919		58.9 28 04	14.9	0.36	1	N	7098	K
095	N 4921		59.0 28 08	13.7	0.36	5	RCBH	5479	A
096	N 4922		59.0 29 35		1.38	7	R	7376	A [4]
097	N 4923		59.1 28 06	14.7	0.39	1	N	5446	K
098			59.1 28 47	15.3	0.80	5	VB	(8922)	G
099	I 843		59.2 29 24	14.8	1.22	2	RCBH	7518	K
100			59.4 28 09	15.5	0.44	1	N	7626	G3
101			59.4 28 22	15.2	0.45	4	B	5928	G2
102			59.4 29 19	14.8	1.16	5	VB	7027	G
103	N 4926		59.5 27 53	14.1	0.58	1	R	7786	A

Table 1, Continued. Main Table of Observations.

ID	I(alt.)	R.A. (1950)	Dec. (1950)	m_p	R	M	Color	V_o	Source
160104		12 ^h 59 ^m .6	28 ^o 03'	15.4	0.51	4	B	7213	CR
105	N 4927	59.6	28 16	14.8	0.47	1	N	7572	K
106		59.7	27 55	15.1	0.59	7	B	7188	RC
107	A 16	59.7	29 31	14.9	1.37	4	R	7358	A
108		59.8	28 29	15.5	0.57	7	VB	8323E	CR
109		13 ^h 59.8	28 40	15.5	0.67	1	VR	7625	G
110		00 ^m .0	28 30	15.2	0.62	2	N	5733	G
111		00.0	28 32	15.7	0.63	1	N	7149	G
112	I 4106	00.2	28 22	15.5	0.62	3P	NCBH	7454	G
113	N 4929	00.3	28 18	14.9	0.63	1	N	6353	CR
114		00.3	28 39	15.6	0.75	2	N	7454	G
115		00.4	28 07	15.4	0.66	1	N	8180	G
116	I 4111	00.5	28 20	15.7	0.68	1	N	7904	G
117		00.6	26 47	15.7	1.62	1	B	5970E	G
118	N 4931	00.6	28 17	14.4	0.69	2	B	5839	K
119		00.8	28 50	15.2	0.94	2	N	6931	CR
120	N 4934	00.9	28 17	15.0	0.76	2	B	6104	G
121		01.0	26 49	15.5	1.63	3P	NCBH	6729	G
122	N 4943	01.4	2821	15.6	0.88	1	B	5751	G
123	I 4133	01.5	28 15	15.4	0.89	1	N	6342	G
124A	N 4944	01.5	28 28		0.92	1	B	7009	A
124B						1	VB		
124C						1	VB		
125		01.8	28 31	15.4	1.00	1	R	5984	G
126		02.0	26 56	15.3	1.65	1P	B	10820E	G
127		02.0	27 34	15.5	1.21	7	VB	5577E	G2
128		02.0	29 05	15.3	1.31	1P	VB	8066E	CR
129	N 4952	02.6	29 23	13.6	1.60	1	N	5866	A
130	N 4957	02.8	27 50	14.2	1.25	1	N	6995	K
132		03.0	29 34	15.5	1.80	2	B	7176	G
134	N 4961	03.3	28 00	13.5	1.31	6	VB	2574	A
135		03.6	28 51	15.5	1.48	1	N	8010	G
136		03.6	29 33	15.0	1.88	1	B	8000	G
137A	N 4966	03.9	29 20		1.79	5	VB	7098E	K
137B						2	VB		

Table 1, Continued. Main Table of Observations.

ID	I(alt.)	R.A. (1950)	Dec. (1950)	m_p	R	M	Color	V_o	Source
160138		13 ^h 04. ^m 1	27 ^o 26'	15.7	1.68	1	B	7861	G
139		04.2	29 06	15.0	1.71	7	VB	4854E	G
140	N 4971	04.5	28 48	15.0	1.65	2	R	6394	K
141		04.8	28 18	15.5	1.62	6	VB	6654	G
142A	CT	05.0	26 59		2.09	5	B	11517	CT
142B						1	B		
143		05.2	27 45	15.7	1.78	2	N	6667	G
144		05.6	27 01	15.6	2.18	1P	VB	10352	CT
145		05.6	28 58	15.4	1.93	1	N	7730	G
146		05.8	27 46	15.4	1.90	4	B	7385	G
147	N 4983	06.0	28 35	14.9	1.91	2	R	6647	G
148		06.5	28 27	14.3	2.00	5	RCBH	5986	G
149		06.6	28 18	15.6	2.02	1	N	7276	G
150		06.6	29 18	15.7	2.27	1	VB	9590	G
151	A 19	06.9	29 38	15.1	2.49	1	B	6390E	CR
152	N 5000	07.4	29 10	14.0	2.37	5	RCBH	5729E	CR
159	CT 41	09.7	27 35	15.0	2.79	1	N	6141	CT

NOTE: [1] = Also IC 823.
 [2] = Companion to NE. $V_o = 7127$ (K).
 [3] = Also IC 838, CT 32.^o
 [4] = Peculiar triple galaxy--only counted once in morphological analysis.

radial distance in degrees from the adopted cluster center defined here as midway between NGC 4889 and NGC 4874, i.e., $12^{\text{h}} 57.4^{\text{m}}, 28^{\circ} 14.5'$ (1950). Positional information is not repeated for fainter galaxies in multiple systems, and m_p is not given for multiple systems. Suffixes used in multiple galaxies are a, b, and c in decreasing order of brightness or e (east member) and w (west member) when the brightness order is not so clear. Columns 7 and 8 give morphological and color classifications on systems described later in this chapter. Colors are not given for galaxies with ID numbers less than 160021 for reasons given in Appendix B. Colors such as RCBH are used when there is a conspicuous difference in color between the nucleus and the rest of the galaxy; in this instance the code is Red Center Blue Halo. Column 9 gives the redshift in Km sec^{-1} (reduced to the sun assuming 300 Km sec^{-1} galactic rotation) and column 10 the redshift source [A = Reference Catalogue of Bright Galaxies by de Vaucouleurs and de Vaucouleurs (1964) hereafter referred to as RCBG; C = Tifft in papers already mentioned and in private communication (Tifft 1973b); K = Kintner (1971); CR = Chincarini and Rood (1972a, 1972b); CT = Tifft and Gregory (1972); and G = new observations]. The integer following the letter G in new redshift determinations gives the number of spectra upon which the redshift is based if more than one. Redshifts enclosed in parentheses are somewhat more inaccurate than the rest because they are either based on only one spectral line with nonzero weight in reduction or the comparison spectrum was of poor quality. A discussion of the accuracy of the redshifts is given in Appendix A; typical accuracies are ± 100 to 150 Km sec^{-1} .

Cluster Membership

In general cluster position must be considered along with redshift in discussing cluster membership. This is so because some galaxies in the outer parts of the cluster may have redshifts no farther from the cluster average than some galaxies near the center where the greatest deviations in redshift are found, yet these outer galaxies may have questionable membership. In the present sample, eight galaxies have redshifts that are so high or so low that they clearly should not be considered members. Six of these, numbers 160082, 160126, 130004, 159107, 160142, and 160144, have redshifts between $10,000 \text{ Km sec}^{-1}$ and $14,000 \text{ Km sec}^{-1}$ and a mean m_p of 15.5; the redshifts of numbers 160134 and 159116 lie at about $2,500 \text{ Km sec}^{-1}$, and they have $\langle m_p \rangle = 12.9$. Only one of these eight lies at a radial distance of less than one degree. These galaxies are interesting in their own right for not one of them is morphologically similar to the types of galaxies most often found in clusters--the normal ellipticals and SO's. Two are peculiar ellipticals; the rest are spirals or irregulars.

The remaining 206 galaxies with redshifts are represented in Figure 1 which plots redshift against apparent distance from the cluster center. Three of these galaxies are plotted as triangles and are discussed below.

Object 160150 has a redshift of $9,590 \text{ Km sec}^{-1}$ and a radial distance of over two degrees. If it were located near the cluster center, its redshift would be consistent with cluster membership. However, we will not consider it as a member. In addition, galaxies 160139 and

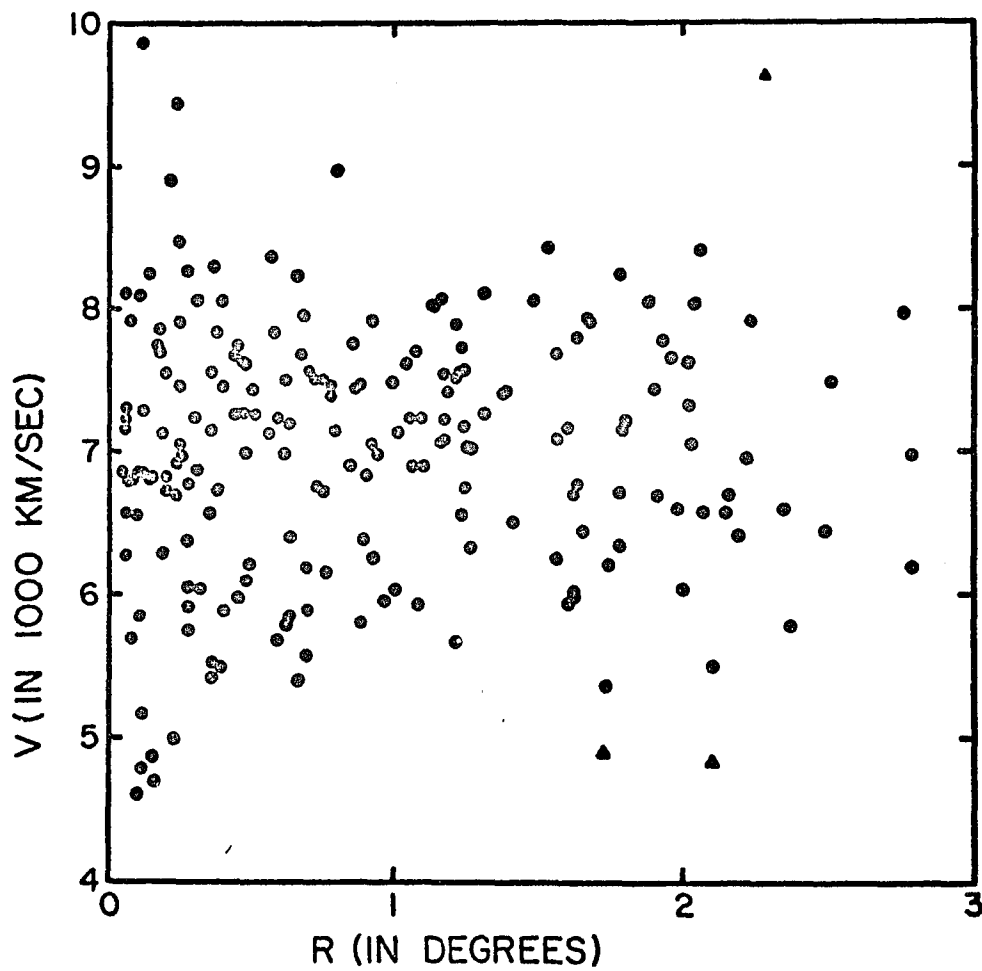


Figure 1. Redshift vs. Apparent Radial Distance. -- Galaxies represented by triangles may not be members of the Coma cluster.

159092 lie at distances greater than 1.7 degrees and have redshifts less than $5,000 \text{ Km sec}^{-1}$. The case for rejecting them is not quite so clear as for 160150, so tests of radial dependence of velocity, velocity dispersion, and rotation will be calculated both with and without their influence.

The nine (or eleven) background and foreground galaxies are consistent with the findings reported in RPKK of ten nonmembers out of a total sample of 102. The area covered by their study was 36 square degrees while that of the present study is roughly 24 square degrees. However, direct comparison cannot be considered only on the basis of area coverage. The Mayall sample, upon which the RPKK study was based, was selected with nuclear brightness and compactness as criteria rather than total magnitude as in this work. In addition, the present sample does not extend far enough west to include the group at $1,000 \text{ Km sec}^{-1}$ redshift that made up most of RPKK's foreground objects. Although some of RPKK's galaxies were fainter than the $m_p = 15.7$ limit used here, the new galaxies were generally fainter than in the earlier sample. Hence one would expect more high redshift galaxies.

Radial Dependence of Redshifts

A test was made to see if redshifts depend upon radial distance from the cluster center; negative results were found. A linear least squares fit gives a slope of $-2 \pm 92 \text{ Km sec}^{-1} \text{ degree}^{-1}$ when 160139 and 159092 were included. The slope is $+41 \pm 91 \text{ Km sec}^{-1} \text{ degree}^{-1}$ excluding the two questionable members.

Velocity Dispersion

The dispersion of redshifts about the mean cluster value has great significance although interpretation of the results often leads to severe conceptual difficulties. It has long been known that the amount of mass necessary to gravitationally bind the Coma cluster galaxies with their large dispersion of redshifts is much greater than the amount of mass present in the visible galaxies. Since the new results do not change the magnitude of σ_v , we defer further comment on the mass discrepancy until the last chapter.

It has been shown before, e.g., RPKK, that the velocity dispersion decreases with distance from the cluster center. Table 2 presents velocity dispersion results for the new sample. The test was run for cells containing 10, 20, 40 and 50 galaxies each. Any leftover galaxies were included in the last cell. The results for cells containing 20 members are presented here; the other tests were either too coarse or followed the statistical fluctuations of the data too closely to be of great use. Columns 1 and 2 give the average radial distance $\langle R \rangle$ (in degrees) and the velocity dispersion σ_v (in Km sec^{-1}) for the case in which galaxies 160139 and 159092 were deleted; the total number $N = 203$ and the mean cluster redshift is 6968 Km sec^{-1} . Columns 3 and 4 give the same data when the two galaxies are included; $N = 205$ and the mean redshift is 6947 Km sec^{-1} .

These findings can be directly compared with those of RPKK. Since the present sample is about twice as large as theirs, we use their results for cell sizes of about ten members. Figure 2 plots their values of σ_v against $\langle R \rangle$ along with the new values in the $N = 205$ case.

Table 2. σ_v vs. R.

R	σ_v	R	σ_v
.08	851	.08	848
.20	974	.20	976
.31	674	.31	671
.46	566	.46	569
.68	688	.68	686
.89	543	.89	545
1.16	512	1.16	515
1.42	477	1.42	484
1.80	599	1.79	685
2.19	1,106	2.21	1,052

Beyond 0.6 degrees the plots agree well and both show the well-known decrease of σ_v with R. Then starting at about $R = 1.80^\circ$, σ_v begins to increase with R. A further decrease beyond the radial limits of this study and to very small values is reported in RPKK. Disagreements between RPKK's and the new results for σ_v near the center are probably caused by the use of Tifft's data which must be considered more accurate than most of the data available to RPKK because Tifft in general used more than one spectrum for each galaxy.

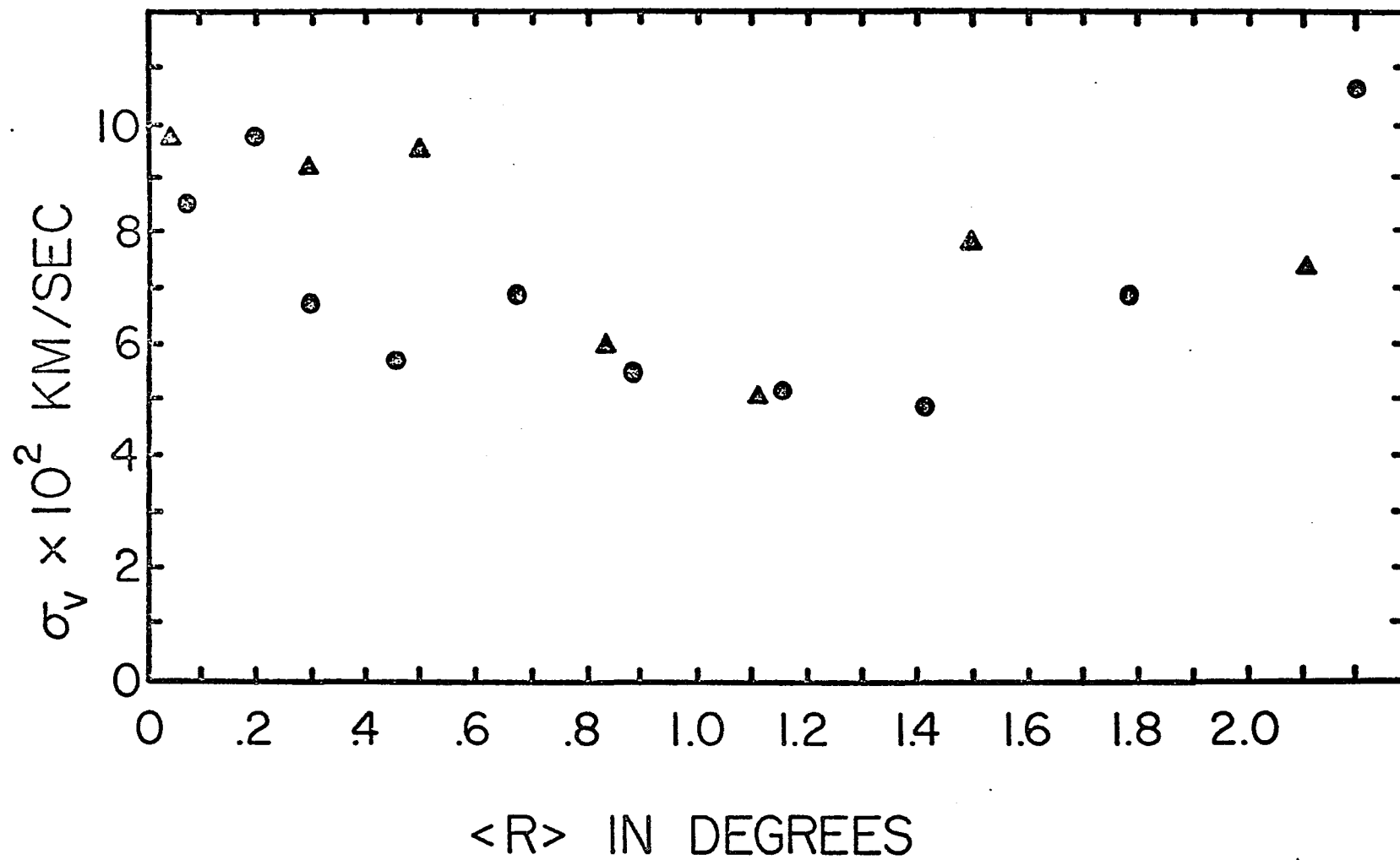


Figure 2. Velocity Dispersion vs. Radius. -- Circles represent new data. Triangles are for data taken from RPKK.

The hump in the σ_v vs. R distribution is certainly real, showing up in both the earlier and this nearly complete sample. This hump cannot be caused entirely by the inclusion of nonmembers. A large part of it comes from the lack of redshifts near the mean as well as from those far from the mean. This can be seen by visual inspection of Figure 1. A more quantitative examination shows that 47 percent of those cluster members lying between 0.5° and 1.4° from the center have redshifts lying within 500 Km sec^{-1} of the cluster average. For the galaxies lying beyond 1.4° , only 33 percent lie within the same range. On the other hand, for both the inner and outer distance ranges, the relative numbers of galaxies lying more than $1,000 \text{ Km sec}^{-1}$ from the mean are nearly the same--21 percent and 25 percent, respectively.

Rotation

As mentioned earlier, Coma is not strictly spherical but rather shows a definite ellipticity. Abell (1963) illustrated this in a study of the distribution of galaxies. One naturally looks to rotation of the cluster as a possible mechanism for flattening. RPKK reported a test for solid body rotation with the galaxies' radial distances projected onto a line with position angle 65° . The results were negative showing a slope of $60 \pm 285 \text{ Km sec}^{-1} \text{ degree}^{-1}$ with the northeast side receding. Only about a dozen of their galaxies had a projected distance greater than one degree.

The present sample was tested in the same manner. Figure 3 shows the distribution of redshifts with projected distance. Galaxies west of the cluster center have positive values of the ordinate.

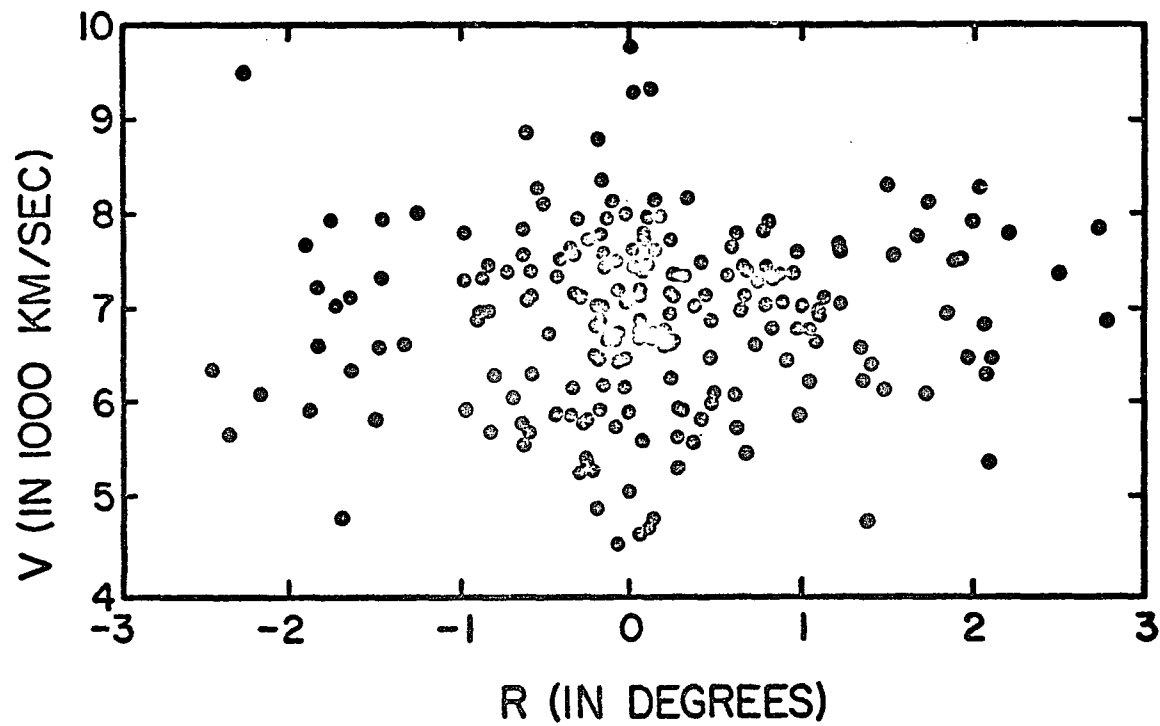


Figure 3. Redshift vs. Projected Distance. -- The point at $V = 9590$, $R = -2.2$ is excluded from the analysis of rotation.

The least squares solution for the slopes are 86 ± 66 (one σ) Km sec^{-1} degree $^{-1}$ for $N = 205$ and 82 ± 66 Km sec^{-1} degree $^{-1}$ for $N = 203$. The major effect of including the two galaxies with questionable membership is to bring the whole solution down from 6945 Km sec^{-1} to 6924 Km sec^{-1} at the center.

Much greater faith can be placed in these findings than in the earlier negative test because four times as many galaxies in this sample project to distances greater than one degree, and it is these galaxies that have the greatest influence on the least squares solution. This can be seen in the vast reduction of the standard deviation of the slopes. It must also be pointed out that the new results are in the opposite sense to the earlier solution. The southwest side is now found to be receding.

The size of the formal error does not impart great confidence in the hypothesis that the cluster is rotating. Indeed, the difference between the solutions for the slopes and zero (no rotation) is less than 1.3 times the standard deviation of the slopes. In addition, the consideration of those galaxies beyond our radial limits with known redshifts does not substantiate our results. Excluding five galaxies with redshifts less than $5,000 \text{ Km sec}^{-1}$ and greater than $4,000 \text{ Km sec}^{-1}$, the solution for the rate of solid body rotation is $+33 \pm 41 \text{ Km sec}^{-1}$ degree $^{-1}$. Let us emphasize, however, the importance of a complete sample for studies of this type since we do not know what selection effects are present in those galaxies beyond our sample.

Another consideration is whether or not solid body rotation is a realistic expectation. It will be shown in Chapter 3 that it should be an excellent approximation to the region of Coma within the present sample. In view of this, the fact that the nearly complete sample indicates rotation, and that a straight line well fits the points in Figure 2, in later discussions we will tentatively accept that Coma is rotating like a solid body. Completion of a redshift sample to even greater distances would be of great interest.

Morphology of Cluster Galaxies

The galaxies in the sample were examined visually with Kitt Peak National Observatory's blink comparator using glass copies of the National Geographic Society-Palomar Observatory Sky Survey (hereafter called the Sky Survey). A numerical morphology classification, M , was made. $M = 1$ represents ellipticals; $M = 3$, SO's; $M = 5$, normal and barred spirals; and $M = 7$ represents peculiar and irregular galaxies. Even number classes refer to galaxies that are intermediate in form or difficult to distinguish. Details of the classification are given in Appendix B. It must be emphasized that this body of data is rough. The small image size and deep exposure of the Sky Survey make accurate morphological classification difficult.

The galaxies were divided into two groups for analysis. One group consists of those galaxies for which $M < 4$, the other with $M > 4$. This grouping does not come from a preconceived idea that E and SO galaxies are necessarily related. Instead, it is only because of the difficulty of distinguishing between these two as opposed to the

relative ease in distinguishing either one from normal spirals and irregulars. Galaxies with $M = 4$ were discarded since better resolution would remove the class entirely, and hopefully equal numbers of E-SO's and spiral-irregulars would be thrown out. In addition, galaxies classified 1p, 2p, or 3p were excluded; these are galaxies that are mostly normal but have small jets or other peculiarities. A small bias is introduced by this since normal spirals with small peculiarities were not excluded but given $M = 6$. However, the bias should not affect radial variations of morphology. Also excluded are galaxies that are clearly not cluster members.

The galaxies were analyzed in rings with the number of spirals and irregulars calculated as a percentage of the total number in the ring. Table 3 gives these results. Column 1 is the inner and outer radii of the rings. Column 2 gives the total number of galaxies, and column 3 the relative number with $M > 4$. In order to consider the possible influence of faint galaxies, columns 2 and 3 are repeated as 4 and 5 but with the fainter companions in multiple systems excluded. This is done because it is not clear about what m_p applies to in such systems.

The monotonic increase in relative numbers of spirals and irregulars (most of this group are spirals) verifies the well-known fact that few spirals are found near the cluster center, more farther out.

Galaxy Colors

A color parameter was assigned each galaxy at the same time that its morphology was classified. The color classes are VB, B, N, R, and

Table 3. Morphology vs. R.

R	N	% M > 4	N	% M > 4
0 ^o .00-0 ^o .50	74	7	70	7
0.51-1.00	47	17	43	18
1.01-1.50	31	23	31	23
1.51-2.00	25	24	24	25
2.01-2.79	16	38	16	38

VR for very blue, blue, neutral, red and very red. Details are again given in Appendix B. The analysis of this color data is limited to $M < 4$ galaxies because the radial increase in relative numbers of $M > 4$ galaxies would induce a color variation with radius since spirals and irregulars are inherently bluer than E and SO galaxies. This would mask any interesting variations of color in the $M < 4$ group. Those galaxies showing large differences between nuclear and halo colors were excluded because it was not clear what the integrated color should be.

Table 4 lists the results. Column 1 again gives the inner and outer radii of the rings. Column 2 is the total number, and column 3 gives the relative number of B or VB galaxies. Columns 4 and 5 again repeat 2 and 3 but with faint members of multiple systems excluded.

A jump in the relative numbers of blue and very blue objects is found at large distances. However, because of the errors inherent in a

Table 4. Color vs. R.

R	N	% B & VB	N	% B & VB
0.00-0.50	68	31	64	30
0.51-1.00	36	25	34	21
1.01-1.50	14	29	14	29
1.51-2.79	17	47	15	44

visual estimation of color, because of the rather small number of galaxies in the outer-most ring, and because the jump is not convincingly large, we must await a more extensive and accurate study in order to have a great deal of confidence that such an effect truly exists.

CHAPTER 3

THEORY

Most of the concepts that will be needed in Chapter 4 to discuss the implications of available observations are quite familiar and do not need amplification. The present chapter, which is devoted to theory, does not attempt to break new ground. Instead, for the most part it extends the work of Gunn and Gott (1972) to a more realistic set of initial conditions.

The major assumptions are the following: (1) the universe is expanding; (2) at an epoch corresponding to about $z = 1000$ the matter and radiation that filled the universe decoupled--the radiation no longer governing the thermal history of the matter; and (3) density perturbations existed on top of a generally uniform background density at the time of decoupling. McCrea (1955) and Callen, Dicke and Peebles (1965) have shown that a Newtonian approximation is valid if the system under consideration is much smaller than the radius of the universe.

Let the radius of a shell of matter be

$$3.1 \quad r(r_i, t) = r_i a(r_i, t).$$

If this shell has no interactions besides gravitational with other shells, then $a(r_i, t)$ satisfies the equation

$$3.2 \quad \left(\frac{da}{dt}\right)^2 = \frac{8\pi G}{3a} \bar{\rho}_i(r_i) + \frac{8\pi G}{3} (\rho_{ci} - \bar{\rho}_i)$$

where $\bar{\rho}(r_i)$ is the average density within the radius r_i at the epoch i , and ρ_{ci} is the critical density of the universe at that epoch.

Equation 3.2 simply states the conservation of energy for each shell. Apart from a factor representing the mass of a shell, the left hand side is twice the kinetic energy; the first term on the right hand side is twice the negative of the potential energy, and the second term is twice the total energy. It can be seen that if $\bar{\rho}(r_i)$ is greater than the critical density, the total energy is negative so that the shell will expand to some maximum radius at which point da/dt will be zero, and the shell will subsequently contract under gravity. If $\bar{\rho}(r_i)$ is less than ρ_{ci} , the shell will expand forever. The critical density marks the transition case in which the expansion is just carried out to infinity at which point there is no velocity.

Letting $\beta \equiv \bar{\rho}_i/\rho_{ci}$ and $\gamma \equiv (\rho_{ci} - \bar{\rho}_i)/\rho_{ci}$ and noting that $\rho_{ci} = 3H_i^2/8\pi G$, H_i being the Hubble parameter at the epoch i , equation 3.2 becomes 3.3

$$3.3 \quad \left(\frac{da}{dt}\right)^2 = H_i^2 (\beta/a + \gamma)$$

For $\gamma < 0$ (i.e., those shells which ultimately collapse) equation 3.3 has the solutions

$$3.3a \quad a = \beta/2\gamma[\cos \psi - 1]$$

and

$$3.4b \quad H_i t = \beta/2\gamma |\gamma|^{1/2} [\sin \psi - \psi], \text{ where } d\psi = |\gamma|^{1/2} \frac{H_i}{a} dt.$$

This shows the form of expansion and subsequent collapse of the shell at $\psi = 2\pi$ or when (from 3.4b)

$$3.5 \quad t_{\text{collapse}}(r_i) = \frac{\pi\beta}{H_i |\gamma|^{3/2}} = \frac{\pi\rho_{ci}^{3/2}}{H_i (\bar{\rho}_{i(n)} - \rho_{ci})^{3/2}}$$

If we now use a realistic form for the density perturbation, we can investigate the effects of equation 3.5 on such a model cluster. Three cases are evidently possible. One is that the background density, ρ_{bg} of the universe was much higher than ρ_{ci} at the epoch corresponding to r_i and that the perturbation existed on top of this. However, we can immediately discount this case because, as we have already noted, the assumption has been made that the universe is still expanding. The second possibility is that the background density was much less than ρ_{ci} . We will not consider this case for the following reason: at least part of the initial Coma perturbation has already collapsed so at least part of the perturbation was denser than ρ_{ci} , but if ρ_{bg} were much less than ρ_{ci} , then the perturbation was much larger in amplitude than the background from which it grew. Such a

situation takes us very far from the linear regime in which the specific form of the perturbation that we will use as a model was derived.

Therefore, the model is one in which the background density was approximately the same as the critical density of the universe at that epoch. For conceptual and computational ease, we will simply take $\rho_{bg} = \rho_{ci}$. We will discuss later what effects a lower value of ρ_{bg} would have since most observations indicate that this is the case.

Field (1972) shows that a density perturbation with $1/r \sin r$ form satisfies the equations governing expansion if the equations are expanded to first order in the perturbed quantities. This function is plotted in Figure 4. Our use of the word shell refers to the volume enclosed by differential elements of the radial coordinate--not the secondary maxima and minima of $1/r \sin r$. We will adopt this giving the expression for density as a function of radius as

$$\rho(r) = \rho_{ci} + \rho_0 \frac{1}{r} \sin r$$

where ρ_0 is the scaling factor of the perturbation and under certain circumstances can be inferred from observations.

The average density within r is

$$\rho(r) = \rho_{ci} + \frac{1}{V_1} \int_{\text{perturbation}} \rho \, dV_1$$

where dV_1 is a volume element. This becomes equation 3.6 when the specific model is used and the integration is performed.

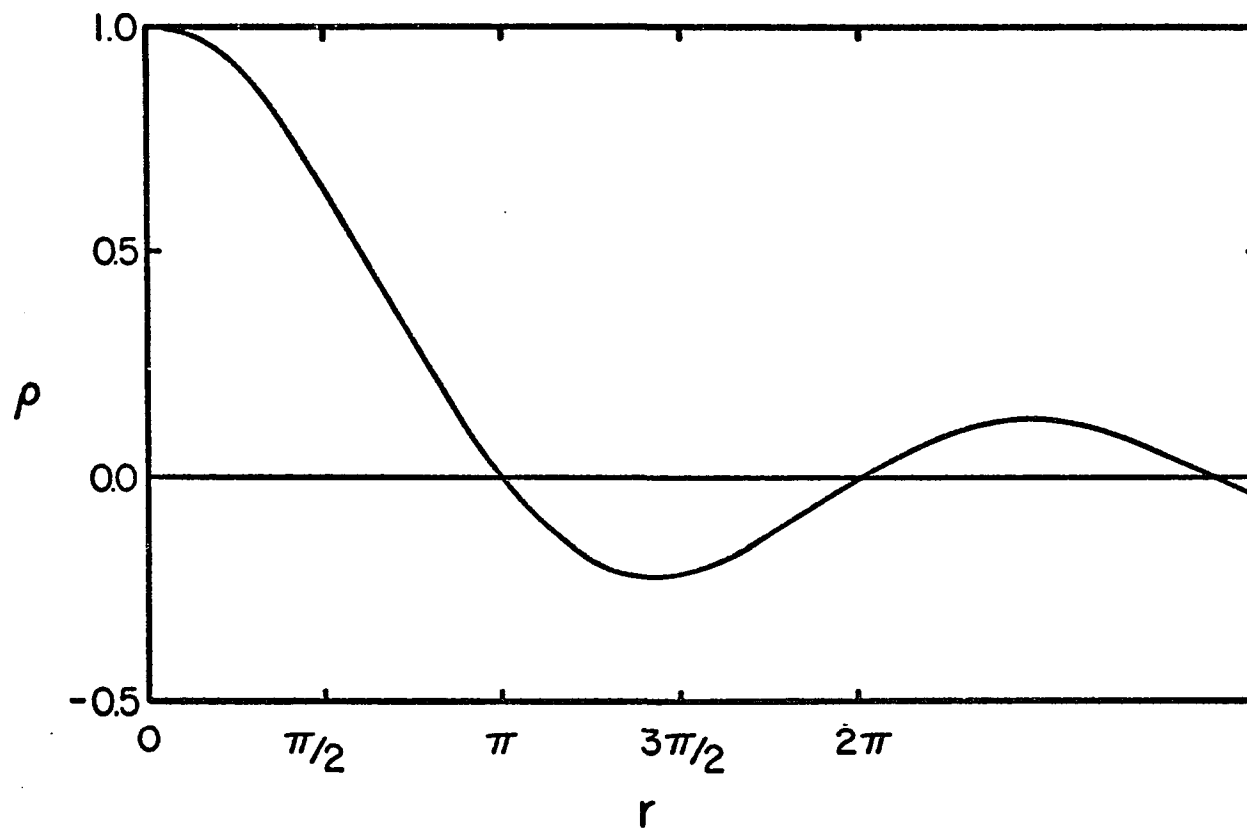


Figure 4. Perturbation Density vs. Radius. -- Units on both axes are arbitrary.

$$\bar{\rho} - \rho_{ci} = \frac{1}{4/3 \pi r^3} \int_0^r 4\pi \rho_0 r \sin r \, dr$$

$$3.6 \quad \bar{\rho} - \rho_{ci} = 3\rho_0 \left[\frac{\sin r - r \cos r}{r^3} \right]$$

Substitution of 3.6 into 3.5 gives the time of collapse as a function of radius.

$$3.7a \quad t_{\text{collapse}}(r_i) = \frac{\pi}{H_i} \left[\frac{\rho_{ci}}{3\rho_0} \frac{r^3}{\sin r - r \cos r} \right]^{3/2}$$

or in particular at $r_i = 0$

$$3.7b \quad t_{\text{collapse}}(r_i = 0) = \frac{\pi}{H_i} \left(\frac{\rho_{ci}}{\rho_0} \right)^{3/2}$$

The form of $\bar{\rho}$ is shown in Figure 5 (actually $\bar{\rho} - \rho_{ci}$ is plotted). We see here that some shells whose radii are initially greater than the first zero of $1/r \sin r$ have $\bar{\rho} > \rho_0$ so even though at that initial point the density was less than the critical density, they still eventually collapse. Beyond this, shells have a lower average internal density and disperse. Still farther yet there is another range of shells that will ultimately collapse and so on.

The logarithm of the time of collapse is plotted against initial radius in Figure 6. The outer regions of the first collapsing zone take as much as 10^2 or 10^3 times as long to collapse as the central regions. This happens for any centrally concentrated model. A shell is considered

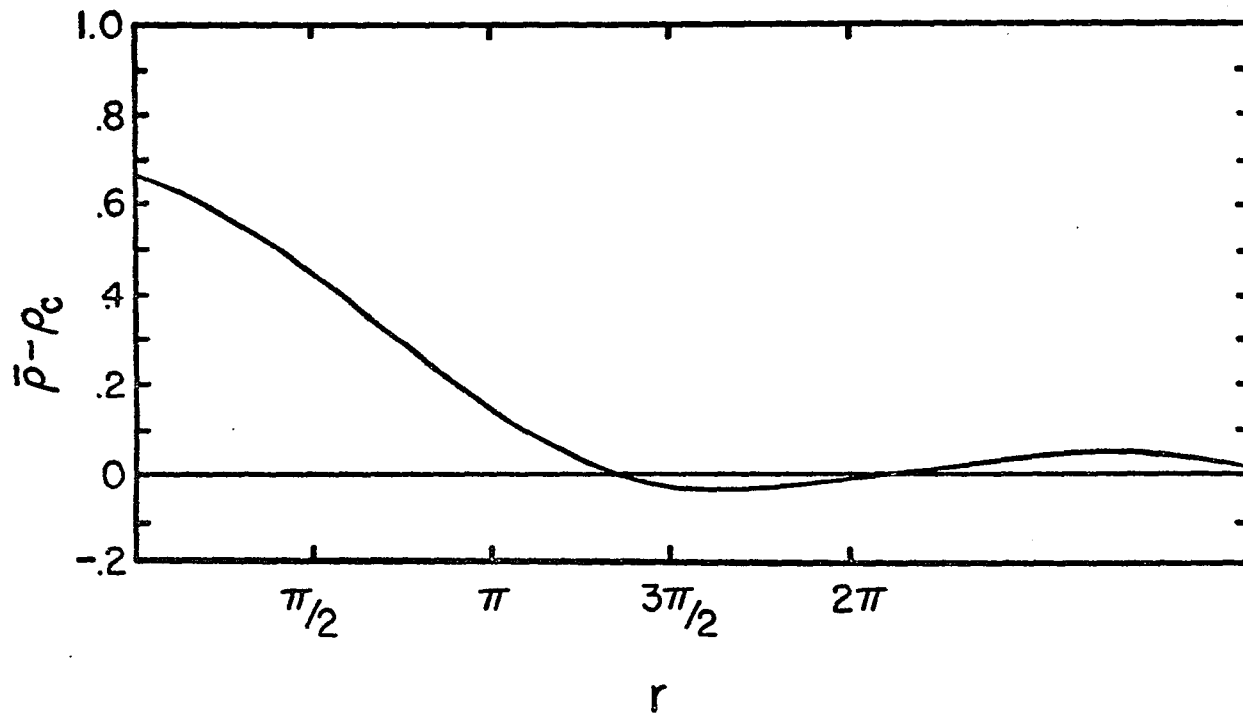


Figure 5. Average Density Within r . ρ_c is the critical density of the universe. Units on both axes are arbitrary.

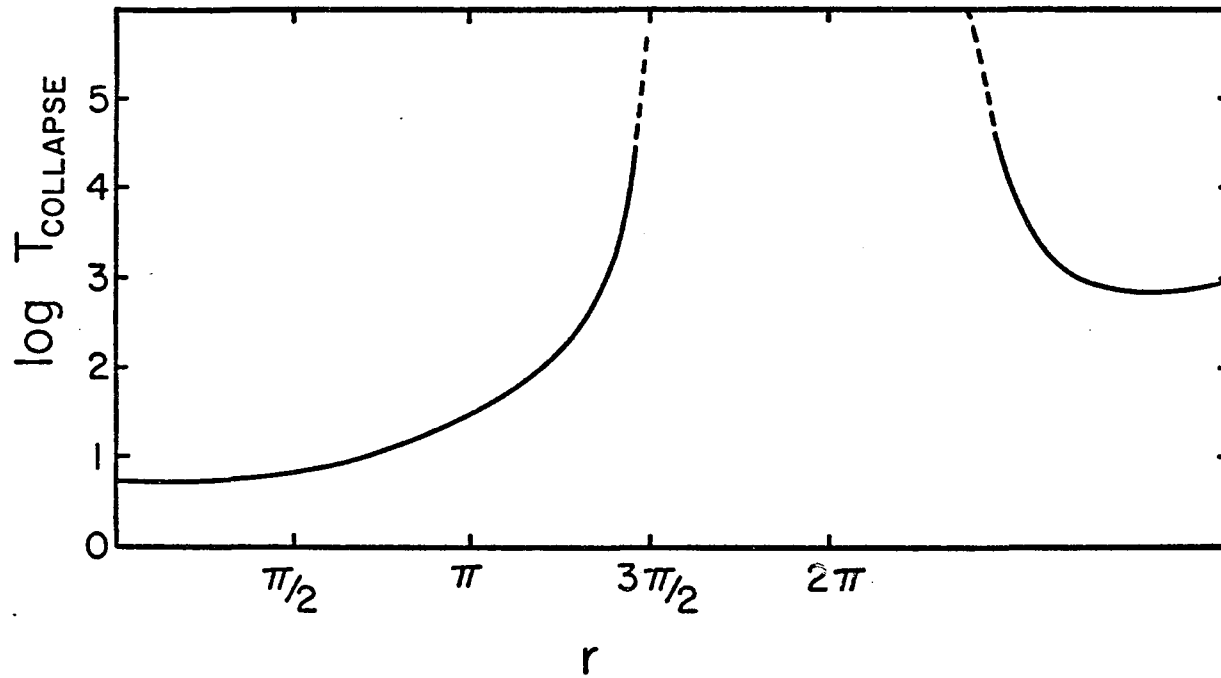


Figure 6. Time of Collapse vs. Radius. -- Units on both axes are arbitrary.

collapsed in the sense of equation 3.5 when it returns to its original radius.

What happens to the shell of matter after its collapse is uncertain. The collapse may be halted in two ways. If the matter is still in gaseous form, collisions with inner shells and subsequent randomization of velocities may be the method. If the matter is already in the form of stars, the violent relaxation method described by Lynden-Bell (1967) would work. The radius at which the shell comes to rest would in general not be the radius at which it is collapsed in the sense of equation 3.5.

Let us investigate the consequences of a model in which the matter is still gas (the other model has been treated by Gott (1973) and will be discussed shortly). This model is not consistent with current ideas of star formation; Eggen, Lynden-Bell and Sandage (1962) have shown that orbital eccentricities of old stars in our galaxy indicate significant star formation had already occurred by the time the galaxy was fully collapsed. Nevertheless, it seems useful to investigate such a possibility since the expected negative results have interest.

Since the outer regions of the cluster take longer to collapse (the time being measured since the decoupling era), the stellar populations of galaxies formed far from the center would be younger than the rest. Whether or not this age difference is significant depends upon the quantity ρ_o/ρ_{ci} . If this ratio of the amplitude of the perturbation to the critical density is large, then the central regions collapse quickly and hence the age difference would not be large. If this ratio

is small, the central regions take longer to collapse, and hence the outer parts may be young compared to the age of the universe, given by the inverse of the Hubble parameter as about 10^{10} years. Let us use 10^8 years for the central collapse as the critical value. If the collapse took much longer, then the outer parts might still be collapsing at the present. From equation 3.7b we can evaluate ρ_o/ρ_{ci} .

$$10^8 = \frac{\pi}{H_i} \left(\frac{\rho_{ci}}{\rho_o} \right)^{3/2}$$

H_i is related to H_o by (c.f. Gunn and Gott, 1972)

$$H_i^2 = 2q_o H_o^2 (1 + z_i)^3$$

Taking $1 + z_i \approx 10^3$ and $2q_o \approx 1$, we find that

$$H_i \approx 3 \times 10^4 H_o \approx 3 \times 10^6 \text{ Km sec}^{-1} \text{ Mpc}^{-1}$$

and therefore

$$\rho_o/\rho_{ci} \approx 1/30$$

It may be possible to use this value as a limit. If observations show galaxies born far from the center to be nearly as old as the ones formed at the center, then 1/30 is a lower limit to ρ_o/ρ_{ci} . Observations to the contrary would make this an upper limit.

Observable Effects of Age Differences

If a significant age difference among galaxies in different parts of the cluster should exist, then observable consequences may result. Tinsley and Spinrad (1972) have examined the color and luminosity evolution over cosmologically significant time scales for a model representing giant elliptical galaxies. The basis for such a model is the synthesis of stellar populations that fit spectroscopic observations of the M 31 inner disk.

Their calculations show that the bolometric magnitude becomes fainter with increasing age. A galaxy ten billion years younger than present galaxies with identical initial makeup would be about 1.6 magnitudes brighter. A two billion year age difference would lead to a brightness difference of about 0.1 magnitude.

The color evolution may be significant. A ten billion year age difference would result in the younger galaxy appearing 0.6 magnitudes bluer in intrinsic B-V, and for a two billion year age difference the younger galaxy would be about 0.1 magnitudes bluer.

The Radial Coordinate

Ideally we would like to relate apparent distances in the Coma cluster to the argument of the function chosen to represent the perturbation. Then we could better judge where to look for galaxies with significant age differences. Two processes may be significant in destroying our ability to match present observations to the original form of the density-radius relation. One of these is radial mixing and

the other process is the continued infall of material into the cluster. This second process will be discussed more fully in the next chapter.

Determinations of the present run of density in Coma differ between workers but generally are of an exponential or modified exponential form. Such functions are much steeper in fall off than is $1/r \sin r$, and this leads to difficulties in applying real distances to the perturbation. For example, the density distribution suggested by Gunn and

Gott (1972), $\rho = \frac{\rho_0 e^{-r/2} a^2}{r^2 + a^2}$, was equated at its half height to $1/r \sin r$

at its half height. This yields a value of $r = \pi$ at 0.25 Mpc suggesting that galaxies formed less than one degree from the cluster center should have been born 10^3 times later than the central galaxies (see Figure 6). Clearly no studies have shown age induced effects for galaxies in such nearby regions, and the evaluation of r should not be taken seriously.

Effects of a Less Dense Background

As noted earlier, current estimates of the density of the universe indicate that the average background density of the universe at earlier cosmological times was less than the critical density. The degree to which the density differed from the critical value depends upon the solution to the problem of the missing mass.

The effects that a less dense background would have on our calculations are of two types. If the background were of the same magnitude as the critical density, then the only effect would be that none of the maxima of $1/r \sin r$ beyond the first zero would be likely to lie above

the critical value. This does not change our arguments because we have not expressly considered these outer shells anyway. The second influence would come if ρ_{bg} were much less than ρ_{ci} . In this case our use of $1/r \sin r$ would no longer be valid since it was derived for small perturbations. However, the true form of the perturbation would appear intuitively to also be one which falls off with radial distance and therefore generate the same qualitative features as the model discussed above.

Gott's Models

Gott (1973) studied computer simulations of the collapse and violent relaxation of axisymmetric rotating systems. The initial conditions were a randomly distributed uniformly dense sphere of objects (his interest was in stellar motions within elliptical galaxies, but it is the same problem as galaxies in a cluster) of radius R_0 . The sphere was then supplied with varying amounts of angular momentum and initial random Maxwellian velocities. The models were then allowed to collapse and the dynamics were examined.

After $3/2T_c$, where $T_c = 2 (R_e^3/GM)^{1/2}$ is twice the free fall time and R_e is given by $R_e = (3GM^2/10E_b)$ where E_b is the binding energy of the cluster, the models reach equilibrium. Isodensity tracings show the expected increase of ellipticity with initial angular momentum.

The first interesting feature is the energy histogram. This shows two peaks. The lower energy peak represents galaxies that were fully relaxed; the higher peak contains galaxies that were outside of the violently relaxing regions either because of initially high

non-radial motions or because they had moved through the core before relaxation commenced. The models with least angular momentum produced the greatest core-halo energy separation.

The second feature is that all models with nonzero angular momentum show solid body rotation to at least $0.5 R_0$ beyond which differential rotation obtains. The models thus confirm Lynden-Bell's (1967) suggested rotation law of

$$\Omega(r) = \frac{\Omega_c}{1 + (r/R_m)^2}$$

where R_m is apparently of the same order of magnitude as R_0 . From the work of Gunn and Gott (1972) we find that $0.5 R_0$ for Coma should be about 3.5 Mpc (over two degrees). Hence we should expect to find solid body rotation throughout most of the present sample.

The velocity dispersion results are most surprising. Gott gives this quantity for all three coordinates, i.e., V_r , V_θ , and V_ϕ . In the center, the motions are isotropic which is expected from an isothermal distribution. The dispersion in all three directions drops off as we move from the center, but at $r \approx 0.6 R_0$, the radial component becomes larger than the other two. Depending upon initial angular momentum, all three components cease decreasing between $r = 0.6 R_0$ and $r = 0.8 R_0$, and in most cases actually increase in this region. This is probably a result of the higher halo energies. Farther out, all dispersions decrease again.

These last results compare with our observed line of sight velocity dispersions. At a given radius r , contributions come from V_{ϕ} for galaxies at r and from V_r and V_{ϕ} for galaxies beyond r . Hence, at some radius less than $0.6 R_o$, halo contributions affect the velocity dispersion, and clearly it will rise if V_r and V_{ϕ} rise sufficiently in value.

Quantitative agreement is lacking, however. Numerical integration of Gott's (1973) non-rotating model shows that V_r or V_{ϕ} would have to be about ten percent greater at their secondary peaks in order for the line of sight dispersion to cease decreasing. The two components would have to be considerably greater to account for the observed secondary rise in dispersion. It is likely that this could be resolved by the addition of greater initial random motions in the models.

Radial Mixing

We must now consider an important question. Does the location at which a galaxy was formed have any bearing on its current location in the cluster?

At Coma's distance one degree of arc corresponds to about 1.6 Mpc. A galaxy traveling at $1,000 \text{ Km sec}^{-1}$ relative to the cluster mean could travel 10 Mpc in 10^{10} years. Such a galaxy therefore could travel through the center and across the 5.6 degree diameter field covered by the present sample in 10^{10} years if it moved in a predominantly radial orbit. However, Gott's study shows that, even in the halo, orbits are far from radial. The radial velocity dispersion rarely exceeds twice either component of the transverse motion. Indeed, Gott followed the

orbits of 20 random galaxies, and they showed box type rather than radial orbits.

Hence, it is likely that radial mixing is not a predominant occurrence, and that most galaxies now found in the outer parts were formed there. The discussion in Chapter 4 will show that the present results are consistent with this picture.

CHAPTER 4

DISCUSSION

Through observations and theoretical studies during the last 20 years, we have learned a great deal about clusters of galaxies using Coma as a prototype. The possibility of rotation of the cluster has been shown for the first time. Yet the idea that Coma could be rotating is not new; it has surely been considered since the earliest realization that the system was somewhat elliptical in shape. An increase of relative numbers of spiral and irregular galaxies with distance from the cluster center has been shown; but, again, this has been suggested for a long time. Perhaps the most surprising result is that the E and SO galaxies found farther out from the center appear to be bluer than the central galaxies of similar type. These new observations along with other recent findings will be discussed in this chapter and an attempt will be made to evaluate their theoretical implication.

The Importance of Faint Members and Nonmembers

The size and total membership of Coma have long been disputed and are important quantities. This study has little bearing on the question of the total radial extent of Coma. Let us just remark that the end has apparently not yet been found (see the first chapter for a short discussion).

The new findings have somewhat more bearing on problems dealing with foreground and background objects. When the RPKK and Tifft and Gregory (1972) papers are considered along with the new work, we find at least three distinct groups of galaxies in the line of sight that are not associated with Coma. To the West are found six galaxies, often as faint as those in Coma, but which have redshifts around $1,000 \text{ Km sec}^{-1}$. These are quite likely dwarfs associated with the group of bright galaxies containing NGC 4448, NGC 4559, and NGC 4656-4657 although these bright galaxies have redshifts a few hundred Km sec^{-1} lower. Two bright galaxies, NGC 4793 and NGC 4961, have redshifts of 2,544 and 2,574 Km sec^{-1} respectively and are very likely associated with each other. Six galaxies mostly lying to the South and West have redshifts ranging from 10,000 to almost 14,000 Km sec^{-1} . One further galaxy, number 160150, may belong to this group on the low redshift side.

On the more subtle question of the membership of galaxies 160139 and 159092, it appears that they make little difference. For example, their inclusion in the solution for the rotation rate changes it very little (from 82 ± 66 to $86 \pm 66 \text{ Km sec}^{-1} \text{ degree}^{-1}$) and their influence on the velocity dispersion is correspondingly small. We therefore adopt as final values those solutions which include the two no longer questionable galaxies. Table 5 summarizes the relevant results. Errors quoted are one standard deviation.

A similar subtle question is whether or not color and morphology statistics are influenced by inclusion of faint members of multiple systems. Their effect on the total color statistics is small but biased.

Table 5. Summary of Redshift Results.

Mean cluster redshift	6947 Km sec ⁻¹
Mean velocity dispersion	712 Km sec ⁻¹
Slope of redshift vs. radial distance	-2 ± 92 Km sec ⁻¹ degree ⁻¹
Rate of solid body rotation	86 ± 66 Km sec ⁻¹ degree ⁻¹

In the three rings listed in Table 4 that did include doubles, all were found bluer than when the faint galaxies were excluded. This agrees with Sandage's (1972) finding that color, especially in U-B, is a function of absolute magnitude with faint galaxies being bluer than bright ones.

The influence of faint galaxies on morphological statistics was even smaller but again biased. In only two rings of Table 3 were the relative numbers of $M < 4$ and $M > 4$ galaxies changed by the faint objects. In both cases, the faint galaxies contributed to a higher incidence of M being greater than 4.

The Kinetic Energy of Rotation

Let us examine the Kinetic Energy that would be present in a solid body at Coma's distance rotating at somewhat over 80 Km sec⁻¹ degree⁻¹. The K.E. is given by $\frac{1}{2}I\omega^2$. The moment of inertia for a flat disk is given by $I = mR^2/2$ and for a homogeneous sphere by $I = 2mR^2/5$. Coma's central concentration would make the coefficient smaller because

I would be weighted more heavily by the higher densities near the center. However, we are interested in obtaining an upper limit for the K.E. so let us use the upper limit of 1/2 for the coefficient in I.

We can now form the ratio of the Kinetic Energy of rotation to the Kinetic Energy caused by individual deviations from the average motion, $K.E._{\sigma}$.

$$\frac{K.E._{rot}}{K.E._{\sigma}} = \frac{\frac{1}{2}I\omega^2}{\frac{1}{2}m\sigma^2}$$

where for the purposes of a rough estimation we will choose σ to be a representative value of the function $\sigma_v(r)$.

$$\frac{K.E._{rot}}{K.E._{\sigma}} = \frac{\frac{mR^2}{2} \left(\frac{V}{2\pi R} \right)^2}{m\sigma^2}$$

V is the linear velocity of rotation at the radius R and m is the mass internal to R . We must assume that the masses in the numerator and denominator refer to the same quantity. Then

$$\frac{K.E._{rot}}{K.E._{\sigma}} = \frac{1}{2} \left(\frac{V}{2\pi\sigma} \right)^2 \approx \frac{1}{80} \left(\frac{V}{\sigma} \right)^2$$

Since σ_v ranges from 500 to 1,000 Km sec⁻¹ and V at 2.79 degrees is only 240 Km sec⁻¹, we see that the K.E. of rotation is 10² or 10³ times smaller than the K.E. of individual motions.

The Dependence of Galaxy Morphology on
Cluster Position

The increase in relative numbers of spiral and irregular galaxies with radial distance seems incontestable. The effect is so strong as to be obvious to the eye on a casual inspection of the Sky Survey and has been mentioned qualitatively many times before.

One possible explanation of such an effect is that spiral galaxies near the cluster center have been stripped of their dust and gas, thus forming SO galaxies. Sandage, Freeman and Stokes (1970) have shown that the characteristic flattening of SO's conforms much more closely to that of true spirals than to that of ellipticals. Similarly, Hodge and Merchant (1966) have shown that the intensity distribution $I(r)$ of SO's follow the exponential law derived for spirals. A steeper form applies to ellipticals (King 1966).

As mentioned earlier, distance scale changes found since Spitzer and Baade's (1951) work have shown that galaxy-galaxy encounters cannot account for a reasonable number of stripped galaxies. Instead, we turn to an intracluster medium. Independent evidence for such a medium comes from the studies of excess light near the cluster center and the diffuse x-ray source which extends over a degree covering the cluster center. Possible indirect evidence concerning galaxy colors will be discussed later in this chapter.

Gunn and Gott (1972) suggest that ram pressure may be effective for stripping if the density of the intracluster medium exceeds 5×10^{-4} atoms cm^{-3} . A re-evaluation of their calculations might use a smaller value than $1,700 \text{ Km sec}^{-1}$ for the rms velocity. This, if halved, would

decrease the calculated ram pressure by three-fourths. However, use of the density in the solar neighborhood of $0.15 M_{\odot} \text{pc}^{-3}$ as given by Mihalas (1968) also brings the restoring force down to about one-fourth the value calculated by Gunn and Gott (1972). Hence the calculation of Gunn and Gott retains roughly the same value.

When we consider Gursky's (1973) value of 10^{-3}cm^{-3} for the density of the hot gas producing x-rays (in a thermal bremsstrahlung model) and the value of $5 \times 10^{-4} \text{atoms cm}^{-3}$ needed to be effective, it seems very likely that such a hot intergalactic medium could remove the dust and gas from a typical spiral galaxy thus producing an SO.

Two points may be raised concerning the distribution of spirals. First, the cluster does not appear to be well mixed since the increase in incidence of spirals is smoothly monotonic and begins near the center. A well-mixed system should show little radial variation. This finding is consistent with Gott's (1973) models. Secondly, we can predict that the relative number of SO's plus normal spirals should be independent of radial distance if the stripping mechanism formed one from the other.

Some caution must be considered even though the picture seems rather self-consistent. As Sandage, Freeman and Stokes (1970) point out, many SO galaxies are found outside of clusters where it becomes difficult to imagine an intergalactic medium of sufficient density to form them by stripping mechanism. Thus such a mechanism appears to be sufficient but not necessary for formation of SO's.

The Possible Change in Color with Distance

It seems useful to consider the implications of a change in the color of $M < 4$ galaxies with radius. Several possible explanations are listed below and then discussed.

1. A type of dynamical sorting has occurred which leaves less massive and hence bluer galaxies on the periphery of the cluster.
2. If E and SO galaxies have different colors on the average, then a radial morphological separation between the two would lead to a color gradient appearing in the $M < 4$ class which includes both types.
3. Intergalactic material in the cluster could redden the central regions.
4. An age effect, such as examined in Chapter 3, could be the cause --implying that the outer galaxies are much younger than those in the center.

Discussion of these possibilities:

1. Equipartition of energy in galaxy-galaxy relaxation would account for less massive galaxies being imparted with greater speeds and hence traveling farther from the center. By assuming then that M/L is relatively independent of L , we would expect that such relaxation would lead to less luminous and hence bluer galaxies being located far from the cluster center. Two problems limit this explanation. First, with the current distance scale, there is little evidence that such processes could relax the cluster

in 10^{10} years. Secondly, as discussed below, we can find little evidence observationally for radial sorting.

In order to see if Coma galaxies are radially sorted according to luminosity and hence mass, the $M < 4$ galaxies were again divided into rings. The innermost ring ranged in radius from $r = 0.0^\circ$ to $r = 0.40^\circ$; the next ranged from 0.41° to 1.50° . These limits were chosen to give approximately equal numbers in each ring. Finally those galaxies beyond 1.51° were considered. For the inner ring $N = 56$ and the average m_p was 15.2; for the middle ring $N = 58$ and $m_p = 15.1$; and for the outer ring $N = 28$ and $m_p = 15.1$. No obvious sorting is seen in these figures. Even consideration of the very brightest galaxies does not necessarily lead to the conclusion that supergiant galaxies are only found in the center. In addition to NGC 4889, the galaxies NGC 4952, NGC 4839, and NGC 4789 are all as bright or brighter than NGC 4874, and they lie at radial distances of 1.60, 0.72, and 1.53 respectively.

2. The average B-V colors of E and SO galaxies in their rest frames were computed from the list of de Vaucouleurs and de Vaucouleurs (1972). The $\langle B-V \rangle$ for 49 E galaxies was 0.87, and for ten SO's it was 0.81. However, the bluest of the SO galaxies, NGC 5548, has a Seyfert nucleus and should be excluded since no Seyferts are found in Coma. For the remaining nine SO's, the $\langle B-V \rangle$ is 0.86. Therefore, the colors of E and SO's are very similar and probably too small a difference exists to detect with visual methods.

3. Reddening by material in our own galaxy seems to be excluded as a possibility since it would have to be caused by a spherical cloud of material centered at the same coordinates as the center of Coma. This is a highly unlikely possibility, and furthermore many studies have shown negligible reddening and absorption at high galactic latitudes.

Reddening by intergalactic material in the cluster itself seems like a much better possibility. To test this we compare the colors of galaxies in the center of Coma to the de Vaucouleurs' (1972) list which includes field galaxies. The Coma E and SO's observed by Sandage (1972) have a $\langle B-V \rangle$ of +0.99; those listed in RCBG have $\langle B-V \rangle = +1.00$, and have an average correction of B-V in the rest frame to observed B-V of +0.12 magnitudes. Adding +0.12 to the rest frame averages for E and SO's from the de Vaucouleurs' list gives $\langle B-V \rangle = +0.99$ and +0.98 for E and SO's respectively.

Thus the center of Coma does not appear to be greatly reddened, but Yahil and Ostriker (1973) show that one would not expect to find more than a few one hundredths of a magnitude of reddening. Their model accounts for the diffuse x-ray source as being thermal bremsstrahlung from gas flowing out of the cluster galaxies. Accompanying this gas outflow would be dust grains which would cause reddening.

Karachentsev and Lypovetskii (1969) have found independent evidence to support the reddening hypothesis. They found

absorption in the B magnitude in 15 clusters which varied smoothly from center to edge. The extinction was found to be smaller in the red which would indicate a λ^{-n} reddening law.

On the other hand, Bahcall and Salpeter (1965, 1966) find that spectra of distant galaxies ($z = 0.46$ and $z = 0.38$) with probabilities of 0.9 and 0.8 respectively of being in line of sight of rich nearby clusters show no evidence of reddening.

4. If the color difference is a result of age effects, then we can estimate the time of collapse of the central regions, as discussed in Chapter 3.

It is difficult with visual estimates to estimate the size of the color difference. Since about half of the outer E and S0's are B or VB and since VB galaxies greatly affect the mean color, let us use a color for the outer $M < 4$ galaxies of $B-V = +0.96$, the mean color of the B class. Hence, the difference between central and outer galaxies seems to be 0.02 or 0.03 magnitudes in $B-V$ which is of the same magnitude as the standard deviation in the mean of each color class (see Appendix B). From the discussion of Tinsley and Spinrad's (1972) work given in Chapter 3, we can estimate an age difference of less than 10^9 years. The luminosity sorting test showed that the central regions may be 0.10 magnitudes fainter in m_p than the outer parts indicating a 2×10^9 year age difference. So according to the model of Tinsley and Spinrad, the outer parts are not vastly younger than the inner ones implying that $t_{\text{collapse}}(r=0)$ is not much in excess of 10^8 years. Therefore $\rho_o = 1/30 \rho_{ci}$ is a lower limit.

Conclusion

This study has provided observational verification of the results of Gott's (1973) work. Coma appears to be rotating, but the rotation is not important energetically. The velocity dispersion has a hump in the outer parts of the cluster, and this is a result of unrelaxed halo galaxies.

New evidence for an intergalactic medium is found in the distribution of spiral galaxies. However, the mass of this medium appears to be less than that of the visible galaxies and therefore does not account for the Virial discrepancy. A possible explanation has been suggested by Ostriker and Peebles (1973). They find that flattened galaxies are unstable unless their halos contain much more mass than is generally thought. They suggest that halos may extend to distances of the size of galaxy separations.

Because of the numerous independent observations of intracluster material, the possible color effects may more likely be considered a result of reddening by the medium than a result of age differences between the central and outer regions. Confirmation of the color effect would indicate that the medium is caused by outflow of material from cluster galaxies rather than infalling matter which would not contain dust grains.

Suggestions for Further Observations

Each of the three observational properties of Coma cluster galaxies tested here has shown interesting variations with respect to the galaxies' positions in the cluster. Two of these tests make use of

data whose accuracy is questionable, and two of the tests show marginal results. Yet it is clear that extension and refinement of the data would be useful. Doubling the number of redshifts that project to a distance of greater than one degree would likely permit a definitive conclusion concerning the rotation of the cluster. Verification would present us with the largest known system with nonzero angular momentum--knowledge of great value in studies of the early stages of the universe.

A larger expenditure of time would be needed to obtain statistics on morphology that are more accurate than those presented here and to determine whether or not any color change really exists. Justification for both studies seems clear. Although the morphological dependence on distance is shown beyond much doubt, refined data would be interesting. An accurate study would also provide data on how the relative numbers of S and SO galaxies vary with distance. This could give us more insight on the origin of SO's. Similarly, if the color change should be verified, then a challenge has been given us--for, no matter what the eventual explanation, this effect would alter many current views of clusters.

Fortunately, the color and morphology studies could be carried out simultaneously, and an ideal telescope now exists for such a study. The 150-inch Mayall telescope of the Kitt Peak National Observatory is very fast, about f2.5 at prime focus, and covers a wide field of about 50 minute diameter with large plate scale. So a program covering a large portion of the cluster could be carried out with maximum speed. Photometry could be done if the fields overlap, if long and short

exposures are made, and if proper photoelectric calibrations are made. Of course, the program would be doubled if a color were to be derived. This is clearly a program of major proportion if done in such a way as to be complete to faint limits and large radial distances.

APPENDIX A

NEW REDSHIFT DETERMINATIONS

All new spectra were taken with the Steward Observatory 90-inch (229 cm) cassegrain spectrograph with an RCA image tube. A 300 line mm^{-1} grating was used, giving dispersions of about 240 \AA mm^{-1} . All plates had the Kodak IIA-0 emulsion. The comparison source was Fe-A.

For several reasons, the spectra were measured by hand on a two-screw Mann 422 comparator. Perhaps the best alternative to a manual comparator is a Grant engine. There are two major difficulties with the latter for spectra such as these. The scanning beam cannot discriminate between photographic grains caused by the galaxy spectrum or comparison source and those resulting from ion or other noise. In addition, some of the galaxies showed lines tilted by rotation since the spectra were unwidened. It would be difficult to use automated methods on such spectra, but an experienced measurer can manually set a crosshair with regard and due compensation for both these and other problems.

Two sets of comparison wavelengths were used because the comparison source current was much higher than normal on the nights of April 21/22, 22/23, 23/24 and 24/25, 1973. The resulting comparison spectrum was therefore somewhat different from the normal.

Table 6 lists the normal and special identifications and adopted wavelengths (in Angstroms) for the comparison lines plus the adopted

Table 6. Rest Wavelengths.

Normal			Late April		Galaxy	
ID	λ	m_{20}	ID	m_{19}	ID	λ
x	-	3764.48	x	3764.76	K	3933.67
3781	3780.84	3780.80	y	3857.62	H	3968.47
a	-	3926.28	a	3925.78	G	4304.40
b	-	3947.26	b	3947.80	4226	4226.73
4014	4013.87	4013.54	c	4104.18	3727	3727.00
4132	4131.73	4131.46			5007	5006.84
4159	4158.58	4159.16			4959	4958.91
4348	4348.11	4348.20			H β	4861.91
4511	4510.73	4510.39			H γ	4340.47
4545	4545.08	4545.42			H δ	4101.74
4657	4657.94	4657.94				
4765	4764.89					
4806	4806.07					
4848	4847.90					
4965	4965.12					
5062	5062.07					

rest wavelengths of the observed galaxy lines. The comparison features x, y, a, b, and c are blends but are useful at these low dispersions if properly calibrated. The wavelengths given under the normal part of the table as the column headed λ are from Moore (1959). Lines to the red of 4657 were used only on spectra showing (OIII) or H β in emission. The column m_{20} was supplied by Tifft (1972c) as calibration for the blends and as further calibration of the characteristics of the Steward system. In the late April spectra, the lines 3781 and 4014 were no longer useful, and the detailed structure of the blends was undoubtedly affected by the increased current. Therefore, on the basis of 19 spectra taken at this time, the blends x, a, and b were recalibrated, and the blends y and c were calibrated. This was accomplished by adjusting m_{19} to minimize the residuals of $\lambda_{\text{calc}} - m_{19}$ about the mean dispersion curve of all previously measured spectra in this project. The table shows that the greatest change was 0.54 A in feature b. The adopted rest wavelengths of the galaxy lines were supplied either by Tifft or taken from de Vaucouleurs and de Vaucouleurs (1967).

Accuracy of the Redshifts

A previous study by the author (Gregory and Connolly 1973) using the same equipment and the same techniques on galaxies of similar magnitudes gave a mean formal internal error of $\pm 110 \text{ Km sec}^{-1}$. From this and the arguments that follow, we adopt an error of ± 100 to 150 Km sec^{-1} for the new redshifts. This is comparable to results at a similar dispersion given by Chincarini and Rood (1972a).

As a further check on accuracy, three objects were re-observed by Tifft (1973b) with the same equipment, and four objects were compared with previous redshift determinations by Kintner (1971), Chincarini and Rood (1972a), or given in RCBG. Galaxy 160127 was also re-observed by Tifft.

Table 7 shows the differences between redshifts determined from plates taken by Gregory and by Tifft (1973b) (922a, 922b, 922c, and 921d --all with abnormal comparison spectra) and from plates taken by Tifft (1973b) or later by Gregory (all with normal comparison spectra). The mean difference is $+30 \text{ Km sec}^{-1}$ with a formal standard deviation of $\sigma = \pm 230 \text{ Km sec}^{-1}$.

Table 8 lists the four galaxies that also have redshift determinations completely independent of Steward Observatory. The columns labelled G-K, G-CR, and G-RCBG give the differences in redshift (in Km sec^{-1}) between those of Gregory and Tifft and those of Kintner (1971), Chincarini and Rood (1972a), and RCBG respectively. Although the number of overlapping objects is small, the clear implication from the two tables is that the new redshifts are consistent internally and with outside investigations except for the results of Kintner which show a large scatter and a possible mis-identification of galaxy 159091. Because of this, Kintner's observations have been given zero weight when other determinations exist for the same object.

Some of the galaxies had more than one spectrum to base the redshift on. These redshifts should therefore be of somewhat higher accuracy than most, but the number of objects is so low that a formal

Table 7. Internal Comparison of Redshifts.

Galaxy	Plate Numbers	Difference in Redshift (Km sec ⁻¹)
160089	922a-946h	+156
160100	922b-948h	-126
	922b-950c	+212
160101	922c-948j	-156
160127	921d-977b	+ 62

Table 8. Comparison of Redshifts with Other Observatories.

Galaxy	G-K	G-CR	G-RCBG
159091	-1081	-73	
159092	+ 216		
159094	+ 437		
160095			+14

value seems meaningless. Three galaxies had only one line that did not receive zero weight during the measuring process. The other lines were either too faint or obstructed by either night sky emission or flaws in the emulsion. Obviously these have lower accuracy, but a formal estimate of the error is impossible.

APPENDIX B

MORPHOLOGY AND COLORS

Morphological Classification

The parameters describing galaxy morphology and color were obtained simultaneously from visual inspection of glass copies of the Sky Survey using Kitt Peak National Observatory's blink comparator. For morphology, a numerical classification system was used; odd numbers represent the types E, SO, S and SB, and Irr and Pec. Even numbers were used for those which were of intermediate form or for which the resolution was not sufficient to classify with any certainty. The classes are listed below with descriptions following.

1. Ellipticals--smooth density gradient; nearly spherical to highly elongated.
2. Intermediate--generally smooth gradient surrounded by very narrow halo; or highly elliptical with some indication of nuclear bulge.
3. SO--bright nucleus surrounded by large halo; discontinuous density gradient between the two.
4. Intermediate--lenticular with definite nuclear bulge; resolution not sufficient to see spiral arms if present.
5. S or SB--normal spirals and barred spirals.

6. Intermediate--spirals with some peculiarity or edge-on disrupted systems.
7. Irregular--irregular or very peculiar.

In addition, some galaxies were classified 1p, 2p, or 3p if the form was not totally disrupted but a jet or some other minor peculiarity was present. Such galaxies are not included in the analysis of Chapter 2.

Accuracy

The exposure times of the Sky Survey were designed to bring out very faint structure. Therefore bright regions are often burnt out. This combined with the rather low plate scale of about 67 arc-seconds mm^{-1} makes accurate morphological classification difficult. Even under ideal conditions such classification can vary between individuals. For example, Rood and Baum (1967) classified NGC 4881 as an E0 galaxy using plates from the 200-inch telescope. De Vaucouleurs in 1971 classified it as an S0 also using a 200-inch plate according to Ables and Ables (1972), who, using tracings from an electronographic plate taken with the U. S. Naval Observatory 40-inch telescope, also call it an S0. In CGCG it is reported to be E1 by Pettit and E1 by Humason, Mayall and Sandage (1956) (hereafter called HMS). In the present study, it is given as $M = 2$.

Differences in classification like the above are certainly of some importance. However, differences that are even much more gross exist. We must ask how many galaxies in the present study that are included in the $M < 4$ group should really have $M > 4$ and vice versa. First, let us look at the 26 galaxies in CGCG that both Pettit and HMS

classified. Several minor discrepancies are present, but there is one galaxy, NGC 4867, that Pettit lists as an E3 but which HMS give as Sa. A similarly large disagreement is found in the HMS classification of IC 4040 as S_{pec} and the present classification of $M = 2$.

Rood made all of the morphological classifications given in RPKK. Seventy-five of these are common to this new sample. Although both studies used plate material from the same telescope, the 48-inch Schmidt, perhaps Rood's classifications should be regarded as somewhat more accurate in view of his extensive experience with the problem of classification from Schmidt plates and because he had access to a high quality blue plate that was not included in the Sky Survey. Of the 75 overlapping galaxies, four (NGC 4738, NGC 4793, NGC 4923, and IC 4040) are large disagreements. Since both Rood and HMS agree on IC 4040, the new classification is probably incorrect. However, for the sake of internal consistency, the list in Table 1 has not been altered.

Five of the 75 galaxies in common are of the intermediate type $M = 4$. Three of these are listed as SO by Rood, and one is SB; another is SO_{pec} . Thus the group with $M = 4$ may likely contain a few more SO's than normal spirals. This probably introduces a bias into the statistics of the relative numbers of $M > 4$ galaxies with distance. This is especially small since only about 11 percent of the total sample is in the $M = 4$ class. Hence the bias should be only a few percent.

Color Classification

The color classifications are perhaps even less accurate than the morphological. Assignment into very blue, blue, neutral, red or

very red colors depended both on change of photographic density and image size during blinking. The Coma cluster lies mainly on two fields of the Sky Survey, and it was hoped that both fields are on a uniform color system. However, comparison between color determinations made for galaxies common to both fields show that those on the field not containing the cluster center (field 159) appear systematically much redder than on the primary field (160). This may be a result of the fact that the plates for the two fields were exposed and developed differently or of either edge effects on the plates or in the blink comparator. The Sky Survey Catalogue of Plates (National Geographic Society 1960) shows a different exposure time for the red plates--45 minutes for 159 and 50 minutes for 160, but this difference is in the opposite sense. One galaxy on field 159, NGC 4692, has a photoelectrically determined $B-V = +0.83$, bluer than average; yet it appears very red. Since this galaxy is not very near the plate edge, a systematic difference over the whole field is suspected. Hence no galaxies in field 159 are included in the color analysis. Also, a machine induced edge effect was found. One light bulb illuminates both plates of the comparator, but it is a couple of inches shorter than the stage. Therefore, the left edge of the left plate and the right edge of the right hand plate are poorly illuminated. This new sample does not extend to the left edge of field 160 but does cover the right edge. Hence the galaxies on the right edge must also be dropped from any analysis. Those dropped are 159106 to 160020 inclusive. The two galaxies on field 130 are also excluded from the statistics.

Although the Sky Survey does not follow the U, B, V system, photoelectric determinations of B-V can serve as a guide to the calibration of the color system used here; the red plate is most sensitive near $H\alpha$, and the blue plate closely follows the international P magnitude--a star with P-V of about +0.7 should appear neutral according to Minkowski and Abell (1963). Fifteen galaxies from the sample, as modified above, have B-V reported in RCBG. Two of these, NGC 4874 and NGC 4889, are classified here as VR. However, because of their very large sizes, small changes in color produce visually impressive changes during blinking. Perhaps their colors should be R instead of VR, but again for internal consistency they have been left unchanged. None of the other VR galaxies have published colors. Table 9 gives the mean B-V for galaxies in each of the remaining classes. The numbers in parentheses beside each color tells how many values contribute to each mean. These means are consistent although the number of calibrating galaxies is small. The four B galaxies overlap a total of 0.06 magnitudes beyond the mean of the N class. The N's overlap a total of 0.03 magnitudes beyond the B mean and 0.01 beyond the R. So, although the mean B-V values are consistent, individual determinations can be considerably in error. A formal solution for the standard deviation about the means based on the ten B and N galaxies yields $\sigma = \pm 0.02$ magnitudes.

Sandage (1972) has published B-V colors for 15 galaxies in common with the sample. Four of these are also common to the galaxies in RCBG. Two, NGC 4889 and NGC 4886, are in excellent agreement, but the other two, NGC 4874 and NGC 4921, differ by 0.07 and 0.08 magnitudes respectively. It is therefore felt that the two lists should be considered

Table 9. Calibration of Colors.

Color	VB(1)	B(4)	N(6)	R(2)
B-V	+0.46	+0.96	+1.00	+1.05

separately. According to Sandage (1972), six galaxies classified as N have a mean B-V of +0.98, and four which were classified as R have a mean of +1.00. Again this shows that the colors for galaxies in two of the classes are consistent. However, there is still considerable scatter within each class, and the means according to the photometry of Sandage and RCBG do not coincide. The standard deviation from Sandage's photometry is $\sigma = \pm 0.03$.

Although the formal value for the standard deviation of colors about the class means is small, ± 0.02 or ± 0.03 , we must realize that the possibility of systematic errors is present and could likely have an important effect on the visually estimated colors.

REFERENCES

- Abell, G. O. 1958 Ap. J. Suppl., 3, 211.
- Abell, G. O. 1962 Problems of Extragalactic Research, ed. G. C. McVittie (New York: Macmillan Co.), p. 213.
- Abell, G. O. 1963 A. J., 68, 271.
- Ables, H. D. and Ables, P. B. 1972 A. J., 77, 642.
- Bahcall, J. N. and Salpeter, E. E. 1965 Ap. J., 142, 1677.
- Bahcall, J. N. and Salpeter, E. E. 1966 Ap. J., 144, 847.
- Bautz, L. P. and Morgan, W. W. 1970 Ap. J. (Lett.), 162, L149.
- Callen, C., Dicke, R. H., and Peebles, P. J. E. 1965 Am. J. Phys., 33, 105.
- Chincarini, G. and Rood, H. J. 1972a A. J., 77, 4.
- Chincarini, G. and Rood, H. J. 1972b A. J., 77, 448.
- de Vaucouleurs, G. and de Vaucouleurs, A. 1964 Reference Catalogue of Bright Galaxies, (Austin: University of Texas Press), RCBG.
- de Vaucouleurs, G. and de Vaucouleurs, A. 1967 A. J., 72, 730.
- de Vaucouleurs, G. and de Vaucouleurs, A. 1972 Memoirs Royal Astr. Soc., 77, 1.
- Eggen, O. J., Lynden-Bell, A. and Sandage, A. R. 1962 Ap. J., 136, 748.
- Field, G. B. 1974 in Stars and Stellar Systems, Vol. 9, ed. A. and M. Sandage (Chicago: University of Chicago Press).
- Gott, J. Richard III. 1973 Ap. J., 168, 481.
- Gregory, S. A. and Connolly, L. P. 1973 Ap. J., 182, 351.

- Gunn, J. E. and Gott, J. R. 1972 Ap. J., 176, 1.
- Gursky, H. 1973 Pub. Astr. Soc. Pac., 85, 493.
- Hodge, P. W. and Merchant, A. N. 1966 Ap. J., 144, 875.
- Humason, M. L., Mayall, N. U. and Sandage, A. R. 1956 A.J., 61,
97, HMS.
- Karachentsev, I. D. and Lipovetskii, V. A. 1969 Sov. Astron.-AJ, 12, 909.
- King, I. R. 1966 A. J., 71, 64.
- Kintner, E. C. 1971 A. J., 76, 409.
- Lynden-Bell, D. 1967 MNRAS, 136, 101.
- Mayall, N. U. 1960 Ann. d'ap., 23, 344.
- McCrea, W. H. 1955 A. J., 60, 271.
- Mihalas, D. 1968 Galactic Astronomy (San Francisco: W. H. Freeman).
- Minkowski, R. L. and Abell, G. O. 1963 in Stars and Stellar Systems,
Vol 3, ed. K. A. Strand (Chicago: University of Chicago Press).
- Moore, C. 1959 A Multiplet Table of Astrophysical Interest (Washington,
D.C.: National Bureau of Standards).
- National Geographic Society, Palomar Observatory Sky Survey Catalogue
of Plates. 1960 California Institute of Technology, Pasadena.
- Omer, G. C., Page, T. L., and Wilson, A. G. 1965 A. J., 70, 440.
- Ostriker, J. P. and Peebles, P. J. E. 1973 Ap. J., 186, 467.
- Philip, A. G. Davis and Sanduleak, N. 1969 Pub. Astr. Soc. Pac.,
81, 53.
- Rood, H. J. and Baum, W. A. 1967 A. J., 72, 398.
- Rood, H. J. and Baum, W. A. 1968 A. J., 73, 442.
- Rood, H. J., Page, T. L., Kintner, E. C., and King, I. R. 1972 Ap. J.,
175, 627, RPKK.
- Rood, H. J. and Sastry, G. N. 1971 Pub. Astr. Soc. Pac., 83, 813.
- Sandage, A. 1972 Ap. J., 176, 21.

- Sandage, A., Freeman, K. C., and Stokes, N. R. 1970 Ap. J., 160, 831.
- Spitzer, L. and Baade, W. 1951 Ap. J., 113, 413.
- Tifft, W. G. 1972a Ap. J., 175, 613.
- Tifft, W. G. 1972b Steward Obs. Preprint No. 45.
- Tifft, W. G. 1972c Private Communication, Tucson, Arizona.
- Tifft, W. G. 1973a Ap. J., 179, 29.
- Tifft, W. G. 1973b Private Communication, Tucson, Arizona.
- Tifft, W. G. and Gregory, S. A. 1972 Ap. J., 181, 15.
- Tifft, W. G., Rood, H. J., Gregory, S. K., and Mahtarakis, P. Z. 1974
in preparation.
- Tinsley, B. M. and Spinrad, H. 1972 Astrophys. and Space Science, 12,
118.
- Welch, G. A. and Sastry, G. N. 1971 Ap. J. (lett.), 169, L3.
- Willson, M. A. G. 1970 MNRAS, 151, 1.
- Yahil, A. and Ostriker, J. P. 1973 Ap. J., 185, 787.
- Zwicky, F. 1957 Morphological Astronomy (Berlin: Springer-Verlag).
- Zwicky, F. and Herzog, E. 1963 Catalog of Galaxies and of Clusters of
Galaxies, Vol. 2 (Pasadena: California Institute of Technology),

CGOG.